Directed Synthesis of the Triangular Mixed-Metal Cluster H2RhRe2CP*(CO)(9): Ligand Fluxionality and Facile Cluster Fragmentation in the Presence of CO, Halogenated Solvents, and Th...

ARTICLE *in* ORGANOMETALLICS · DECEMBER 2009

Impact Factor: 4.13 · DOI: 10.1021/om9007407

ORGANOMETALLICS
Article

Organometallics **2010,** *29,* 61–75 61
DOI: 10.1021/om9007407

Directed Synthesis of the Triangular Mixed-Metal Cluster $H_2RhRe_2Cp^*(CO)_9$: Ligand Fluxionality and Facile Cluster Fragmentation in the Presence of CO, Halogenated Solvents, and Thiols

Shih-Huang Huang,[†] William H. Watson,[‡] Carl J. Carrano,[§] Xiaoping Wang,[∥] and Michael G. Richmond*,[†]

[†]*Department of Chemistry, University of North Texas, Denton, Texas 76203,* [‡]*Department of Chemistry, Texas Christian University, Fort Worth, Texas 76102,* [§]*Department of Chemistry and Biochemistry, San Diego State University, San Diego, California 82182, and* [∥]*Neutron Scattering Science Division, Oak Ridge National Laboratory, Oak Ridge, Tennessee 37831*

Received August 24, 2009

The reaction of $H_2Re_2(CO)_8$ (**1**) with $Cp^*Rh(CO)_2$ (**2**) in refluxing hexane affords the mixed-metal clusters $H_2RhRe_2Cp^*(CO)_9$ (**4**, major product), $HRh_2ReCp^*_2(CO)_6$ (**5**), and $HRhRe_3Cp^*(CO)_{14}$ (**6**). **4** and **5** are electron-precise 48e clusters and display triangular metallic cores, while **6** contains 64 valence electrons and exhibits a spiked-triangular core having a pendant $Re(CO)_5$ moiety. Heating **1** with $Cp^*_2Rh_2(CO)_2$ (**3**) gives **4** and **5** as the principal products, in addition to $H_2Rh_2Re_2Cp^*_2(CO)_8$ (**7**) in low yield. Cluster **7** possesses 60e and contains a tetrametallic core with two face-capping CO and hydride groups. Heating **4** under CO leads to cluster fragmentation and formation of $Re_2(CO)_{10}$ and **2** in essentially quantitative yield, as assessed by IR spectroscopy. The kinetics for the fragmentation of **4** in toluene under CO have been investigated over the temperature range 325−349 K by UV−vis spectroscopy. On the basis of the first-order rate constants and the Eyring activation parameters ($\Delta H^{\ddagger}$ = 25.0(8) kcal/mol; $\Delta S^{\ddagger}$ = −2.6(3) eu), a rate-limiting step involving a polyhedral opening of **4** is supported. **4** is thermally and photochemically sensitive, and reactions conducted in the presence of chlorinated solvents furnish the face-shared bioctahedral compound $Cp^*Rh(\mu\text{-}Cl)_3Re(CO)_3$ (**8**). Heating **4** and H_2S in benzene at ca. 60 °C furnishes the 48e triangular cluster $S_2Rh_3Cp^*(CO)_4$ (**9**), which contains two $Rh(CO)_2$ moieties and two face-capping sulfide groups. The reaction of **4** with *p*-methylbenzenethiol gives the sulfido-bridged dimer $Cp^*Rh(\mu\text{-}SC_6H_4Me\text{-}p)_3Re(CO)_3$ (**11**). The dinuclear compounds $Cp^*Rh(\mu\text{-}Cl)(\mu\text{-}SC_6H_4Me\text{-}p)_2Re(CO)_3$ (**10**) and **11** are formed when **8** is allowed to react with *p*-methylbenzenethiol. Treatment of **8** and **10** with excess *p*-methylbenzenethiol yields **11** at elevated temperature in toluene. Compounds **4**−**11** have been isolated and fully characterized by IR and NMR spectroscopy and by X-ray crystallography. The reactivity displayed by **4** is contrasted with that of the known indenyl-substituted cluster $H_2Re_2Ir(\eta^5\text{-ind})(CO)_9$ prepared earlier by Shapley and co-workers.

Introduction

Numerous industrial processes employ bimetallic alloy or nanoparticle catalysts for the production of commodity chemicals because of the experimentally determined catalytic activity superior to that of the corresponding reactions conducted with the individual monometallic components.[1] The enhanced properties exhibited by such mixed-metal systems are defined, typically, by increased reaction rates and/or altered product distributions. Given the general difficulty associated with the mechanistic study of such heterogeneous systems, researchers continue to utilize homogeneous mixed-metal compounds as models that can, at least in theory, provide crucial insight into the origins of cooperative metal reactivity in heterogeneous systems.[2] The synergistic effect displayed by certain solution-soluble di- and polynuclear metal compounds in hydrogenation,[3] hydroformylation,[4]

*To whom correspondence should be addressed. Tel: 940-565-3548. E-mail: cobalt@unt.edu.

(1) (a) Burda, C.; Chen, X.; Narayanan, R.; El-Sayed, M. A. *Chem. Rev.* **2005**, *105*, 1025. (b) Thomas, J. M.; Johnson, B. F. G.; Raja, R.; Sankar, G.; Midgley, P. A. *Acc. Chem. Res.* **2003**, *36*, 20. (c) Johnson, B. F. G. *Coord. Chem. Rev.* **1999**, *192*, 199. (d) Topsøe, H.; Clausen, B. S.; Massoth, F. E. In *Hydrotreating Catalysis, Science and Technology*; Anderson, J. R., Boudart, M., Eds.; Springer: Berlin, 1996; Vol. *11*. (e) Sinfelt, J. H. *Bimetallic Catalysis: Discoveries, Concepts, and Applications*; Wiley: New York, 1983. (f) Pignolet, L. H. In *Catalysis by Di- and Polynuclear Metal Cluster Complexes*; Adams, R. D., Cotton, F. A., Eds.; Wiley-VCH: New York, 1998; Chapter 3.

(2) Rothenberg, G. *Catalysis: Concepts and Green Applications*; Wiley-VCH: Weinheim, Germany, 2008.

(3) (a) Adams, R. D.; Barnard, T. S.; Li, Z.; Wu, W.; Yamamoto, J. H. *J. Am. Chem. Soc.* **1994**, *116*, 9103. (b) Adams, R. D.; Barnard, T. S. *Organometallics* **1998**, *17*, 2885.

(4) (a) Li, C.; Chen, L.; Garland, M. *J. Am. Chem. Soc.* **2007**, *129*, 13327. (b) Li, C.; Chen, L.; Garland, M. *Adv. Synth. Catal.* **2008**, *350*, 679. (c) Liu, G.; Li, C.; Guo, L.; Garland, M. *J. Catal.* **2006**, *237*, 67. (d) Li, C.; Widjaja, E.; Garland, M. *Organometallics* **2004**, *23*, 4131. (e) Li, C.; Widjaja, E.; Garland, M. *J. Am. Chem. Soc.* **2003**, *125*, 5540.

Published on Web 12/10/2009

silaformylation,[5] and C−C bond coupling reactions[6] provides unequivocal proof for cooperative catalytic activity between the dissimilar metals. Two recent and undisputed paradigms involving bimetallic synergism include Adams' platinum-promoted alkyne insertion into the metal−hydride bond in $HPtOs(CO)_4(SnPh_3)(PBu^t_3)$ and Garland's kinetic and spectroscopic demonstration of the heterobimetallic system composed of $HRe(CO)_5$/Rh(acyl)$(CO)_4$ that catalytically gives aldehydes and $RhRe(CO)_9$ upon activation of molecular hydrogen.[4a,b,7] Equation 1 depicts the regiospecific alkyne insertion observed in the former reaction.

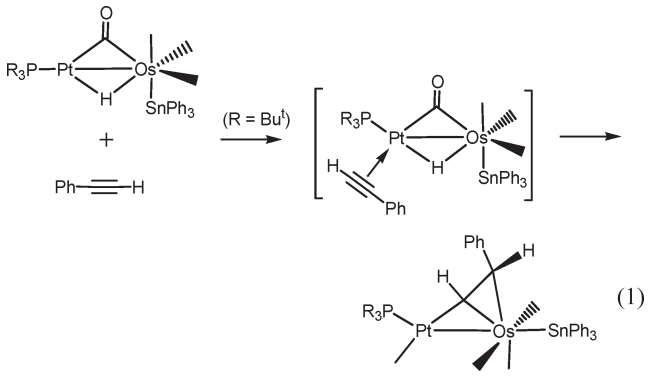

(1)

We have published several reports describing the fluxional behavior of unsaturated diphosphines at homometallic trinuclear clusters and the dynamics for reversible ortho metalation that can accompany diphosphine isomerization at elevated temperatures.[8] Scheme 1 illustrates the sequence of events displayed by the triosmium cluster $Os_3(CO)_{10}$(bpcd) (where bpcd = 4,5-bis(diphenylphosphino)-4-cyclopenten-1,3-dione). The hydride cluster produced by ortho metalation, namely $HOs_3(CO)_9[\mu$-PhP(C_6H_4)C=C(PPh_2)C(O)CH_2C(O)], readily regenerates the chelated cluster 1,1-$Os_3(CO)_{10}$(bpcd) when it is heated under CO. The reductive coupling process was thoroughly investigated, and C−H bond formation was shown to exhibit an inverse equilibrium isotope effect (EIE) through a combination of kinetic and equilibrium measurements. The isotope data strongly support the involvement of an intermediate aryl π-complex prior to the rate-limiting formation of the unsaturated cluster 1,1-$Os_3(CO)_9$(bpcd), which undergoes a rapid reaction with added CO to regenerate 1,1-$Os_3(CO)_{10}$(bpcd). Extrapolation of these homometallic studies to heterometallic systems would allow us to probe the regiochemical aspects associated with the formation of the diphosphine-chelated cluster and the subsequent ortho-metalation step. Moreover, should site-specific ortho metalation be observed in a heterometallic cluster, the data could be contrasted with appropriate metalation reactions observed in mononuclear compounds and the effect of the "cluster template" on the ortho metalation readily assessed. The "cluster template" concept has, in fact, been demonstrated in site-selective oxidative-addition reactions of allyl bromide and Ph_3SiH at the octanuclear carbide cluster $[Re_7C(CO)_{21}Ir(coe)(CO)]^{2-}$ (where coe = cyclooctene). Here regiospecific substrate activation occurs at the iridium center to furnish exclusively the clusters $[Re_7C(CO)_{21}Ir(\eta^3$-allyl)$(CO)]^-$ and $[Re_7C(CO)_{21}IrH(SiPh_3)(CO)]^{2-}$. Whereas control experiments revealed a reactivity parallel with that of the mononuclear compound Ir(η^5-ind)(cod)(CO), the corresponding CpIr(coe)(CO) derivative was found to be inert under analogous conditions.[9]

Unlike their homometallic counterparts, the directed synthesis of mixed-metal clusters is far from trivial.[10] It is not uncommon for such reactions to be plagued by low yields and/or product mixtures necessitating time-consuming and tedious chromatographic separations. The situation is further exacerbated if the desired heterometallic cluster is unstable and irreversibly bound to the stationary phase during chromatographic separation. Accordingly, a major prerequisite in any mechanistic study dealing with ligand activation at a heterometallic cluster involves the ready availability of the starting cluster in amounts that will facilitate the associated spectroscopic, physical, and kinetic analyses. Our interest in the title heterometallic cluster $H_2RhRe_2Cp^*(CO)_9$ stems, in part, from the earlier report by Shapley and co-workers on the indenyl-substituted cluster $H_2Re_2Ir(\eta^5$-ind$)(CO)_9$, which may be prepared in 80% yield from $H_2Re_2(CO)_8$ and Ir$(CO)(\eta^2$-coe$)(\eta^5$-ind) as shown in eq 2.[11] The dinuclear compound $H_2Re_2(CO)_8$ is a suitable precursor for the directed synthesis of MRe_2 clusters because it is easily prepared in 0.2−0.4 g amounts from $Re_2(CO)_{10}$ and it is reactive in cluster aggregation scenarios due to its intrinsic unsaturation, features utilized by others for the construction of triangular $PtRe_2$ and $IrRe_2$ clusters as well as polynuclear rhenium clusters.[12,13] Instead of using $H_2Re_2Ir(\eta^5$-ind$)(CO)_9$ in our diphosphine ligand activation studies, we wanted to prepare the unknown $H_2RhRe_2Cp^*(CO)_9$ derivative and utilize the presence of the ^{103}Rh nucleus (100% natural abundance and $I = {}^1/_2$) to assist with the NMR interpretation of the reaction products. The choice of the RhRe metallic composition was also guided by reports of bifunctional hydroformylation, hydrogenation, and oxidation

(5) (a) Ojima, I.; Okabe, M.; Kato, K.; Kwon, H. B.; Horváth, I. T. *J. Am. Chem. Soc.* **1988**, *110*, 150. (b) Ojima, I.; Vidal, E.; Tzamarioudaki, M.; Matsuda, I. *J. Am. Chem. Soc.* **1995**, *117*, 6797. (c) Ojima, I.; Donovan, R. J.; Ingallina, P.; Clos, N.; Shay, W. R.; Eguchi, M.; Zeng, Q.; Korda, A. *J. Cluster Sci.* **1992**, *3*, 423.

(6) Shenglof, M.; Molander, G. A.; Blum, J. *Synthesis* **2006**, 111.

(7) Adams, R. D.; Captain, B.; Zhu, L. *J. Am. Chem. Soc.* **2006**, *128*, 13672.

(8) (a) Watson, W. H.; Wu, G.; Richmond, M. G. *Organometallics* **2005**, *24*, 5431; **2006**, *25*, 930. (b) Watson, W. H.; Poola, B.; Richmond, M. G. *J. Organomet. Chem.* **2006**, *691*, 4676. (c) Watson, W. H.; Poola, B.; Richmond, M. G. *Polyhedron* **2007**, *26*, 3585.

(9) Ma, L.; Szajek, L. P.; Shapley, J. R. *Organometallics* **1991**, *10*, 1662.

(10) (a) Beurich, H.; Vahrenkamp, H. *Angew. Chem., Int. Ed.* **1978**, *17*, 863. (b) Geoffroy, G. L. *Acc. Chem. Res.* **1980**, *13*, 469. (c) Stone, F. G. A. *Pure Appl. Chem.* **1986**, *58*, 529. (d) Clark, D. T.; Sutin, K. A.; Perrier, R. E.; McGlinchey, M. J. *Polyhedron* **1988**, *7*, 2297.

(11) Comstock, M. C.; Prussak-Wieckowska, T.; Wilson, S. R.; Shapley, J. R. *Inorg. Chem.* **1997**, *36*, 4397.

(12) (a) Al-Resayes, S. I.; Hitchcock, P. B.; Nixon, J. F. *J. Chem. Soc., Chem. Commun.* **1987**, 928. (b) Beringhelli, T.; Ceriotti, A.; D'Alfonso, G.; Pergola, R. D.; Ciani, G.; Moret, M.; Sironi, A. *Organometallics* **1990**, *9*, 1053. (c) Ciani, G.; Moret, M.; Sironi, A.; Antognazza, P.; Beringhelli, T.; D'Alfonso, G.; Pergola, R. D.; Minoja, A. *J. Chem. Soc., Chem. Commun.* **1991**, 1255. (d) Beringhelli, T.; Ciani, G.; D'Alfonso; Garlaschelli, L.; Moret, M.; Sironi, A. *J. Chem. Soc., Dalton Trans.* **1992**, 1865. (e) Antognazza, P.; Beringhelli, T.; D'Alfonso, G.; Minoja, A.; Ciani, G.; Moret, M.; Sironi, A. *Organometallics* **1992**, *11*, 1777.

(13) (a) Bergamo, M.; Beringhelli, T.; D'Alfonso, G.; Ciani, G.; Moret, M.; Sironi, A. *Organometallics* **1996**, *15*, 3876. (b) Bergamo, M.; Beringhelli, T.; D'Alfonso, G.; Mercandelli, P.; Moret, M.; Sironi, A. *Organometallics* **1997**, *16*, 4129. (c) Bergamo, M.; Beringhelli, T.; D'Alfonso, G.; Mercandelli, P.; Moret, M.; Sironi, A. *J. Am. Chem. Soc.* **1998**, *120*, 2971. (d) Bergamo, M.; Beringhelli, T.; D'Alfonso, G.; Mercandelli, P.; Moret, M.; Sironi, A. *Angew. Chem., Int. Ed.* **1998**, *37*, 2128; **1999**, *38*, 3486. (e) Masciocchi, N.; D'Alfonso, G.; Garavaglia, L.; Sironi, A. *Angew. Chem., Int. Ed.* **2000**, *39*, 4478. (f) D'Alfonso, G. *Chem. Eur. J.* **2000**, *6*, 209. (g) Bergamo, M.; Beringhelli, T.; D'Alfonso, G.; Garavaglia, L.; Mercandelli, P.; Moret, M.; Sironi, A. *J. Cluster Sci.* **2001**, *12*, 223.

Scheme 1

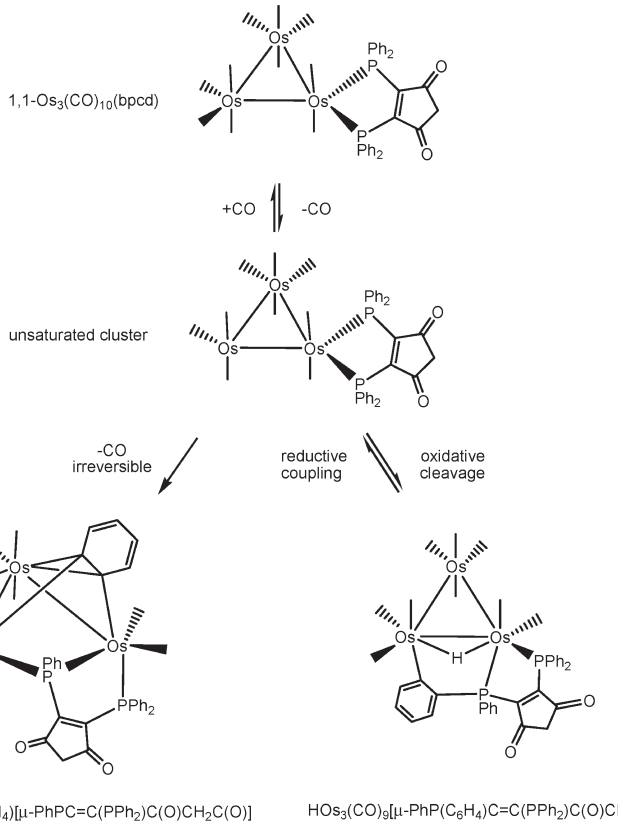

catalysis based on RhRe systems,[4a,b,14] which would allow the targeted $H_2RhRe_2Cp^*(CO)_9$ cluster to be employed as a nanoparticle precursor in future catalysis studies.

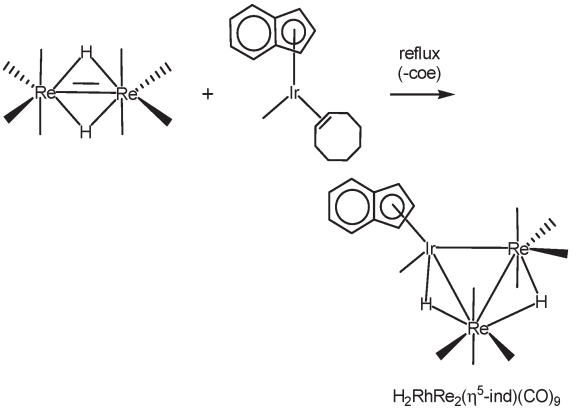

(2)

Herein we report our results on the synthesis of $H_2RhRe_2Cp^*(CO)_9$ (**4**) from $H_2Re_2(CO)_8$ (**1**) with $Cp^*Rh(CO)_2$ (**2**). Accompanying products in this reaction are the metal clusters $HRh_2ReCp^*_2(CO)_6$ (**5**) and $HRhRe_3Cp^*(CO)_{14}$ (**6**), which have been isolated and fully characterized. The targeted cluster **4** has also been prepared by an alternative path starting from **1** and the unsaturated rhodium dimer $Cp^*_2Rh_2(CO)_2$ (**3**). Unexpectedly, **4** undergoes facile decomposition in the presence of added ligands; some of the decomposition products have been isolated, and their identities are discussed within.

Experimental Section

General Methods. The starting materials $H_2Re_2(CO)_8$,[15] $Cp^*Rh(CO)_2$,[16] and $Cp^*_2Rh_2(CO)_2$[17] employed in our studies were synthesized according to established procedures or modifications thereof. The $Re_2(CO)_{10}$ and the hydrated $RhCl_3$ were purchased from Pressure Chemical Co. and the Engelhard Corp., respectively. $[Cp^*RhCl_2]_2$ was prepared from hydrated $RhCl_3$,[18] with the ligand pentamethylcyclopentadiene synthesized by starting from 2-bromo-2-butenes (isomeric mixture),[19] the latter of which was purchased from Aldrich Chemical Co. The chemicals *p*-methylbenzenethiol and $Me_3NO\cdot xH_2O$ were also purchased from Aldrich; the latter chemical was used in the anhydrous form after the waters of hydration were removed by azeotropic distillation using benzene. The ^{13}CO (>99% ^{13}C) used in the preparation of the ^{13}CO-enriched $H_2Re_2(CO)_8$ and $Cp^*Rh(CO)_2$ was purchased from Isotec, Inc., and the D_2 (>99.7%) that was used in the synthesis of **1**-d_2 was obtained from Matheson Tri-Gas. **1**-d_2 was prepared by photolysis of $Re_2(CO)_{10}$ under D_2 and was employed in the synthesis of **4**-d_2 after recrystallization from hexane (−30 °C).[20] All reaction

(14) (a) Trivedi, B. C.; Grote, D.; Mason, T. O. *J. Am. Oil Chem. Soc.* **1981**, *58*, 17. (b) Baker, R. T.; Glassman, T. E.; Ovenall, D. W.; Calabrese, J. C. *Isr. J. Chem.* **1991**, *31*, 33. (c) Koussathana, M.; Vamvouka, N.; Verykios, X. E. *Appl. Catal., A* **1993**, *95*, 211. (d) Haupt, H.-J.; Wittbecker, R.; Flörke, U. *Z. Anorg. Allg. Chem.* **2001**, *627*, 472. (e) Zhao, S.; Hu, X. D.; Tolle, P.; David, P.; Rogers, D. B. U.S. Patent WO2008011282.

(15) Comstock, M. C.; Shapley, J. R. *Inorg. Synth.* **2002**, *33*, 208.

(16) Compound **2** was prepared in relatively good yield using the methodology outlined for the synthesis of the corresponding iridium analogue $Cp^*Ir(CO)_2$. See: Ball, R. G.; Graham, W. A. G.; Heinekey, D. M.; Hoyano, J. K.; McMaster, A. D.; Mattson, B. M.; Michel, S. T. *Inorg. Chem.* **1990**, *29*, 2033.

(17) Herrmann, W. A.; Plank, J.; Bauer, C.; Ziegler, M. L.; Guggolz, E.; Alt, R. *Z. Anorg. Allg. Chem.* **1982**, *487*, 85.

(18) White, C.; Yates, A.; Maitlis, P. M. *Inorg. Synth.* **1992**, *29*, 228.

(19) Threlkel, R. S.; Bercaw, J. E. *J. Organomet. Chem.* **1977**, *136*, 1.

(20) For a report on the small-scale synthesis of **1**-d_2 starting from **1**-d_0 and using D_2O and Florisil, see: Andrews, M. A.; Kirtley, S. W.; Kaesz, H. D. *Inorg. Chem.* **1977**, *16*, 1556.

Table 1. IR and NMR Spectroscopic Data for Compounds 4−11[a,b]

compd	IR, cm^{-1}	^1H NMR, δ
4	2100 (s), 2067 (s), 2032 (w), 2008 (vs), 1996 (s), 1977 (m), 1963 (s), 1941 (m)	1.54 (s, 15H, Cp*), −15.96 (d, 1H, J_{Rh-H} = 26 Hz), −16.04 (s, 1H)
5	2057 (s), 1968 (vs), 1936 (s), 1804 (m)	1.76 (s, 30H, Cp*), −18.81 (d, 1H, J_{Rh-H} = 32 Hz)
6	2145 (w), 2113 (m), 2078 (m), 2048 (vs), 2016 (vs), 1993 (vs), 1977 (s), 1967 (m), 1945 (w), 1932 (m), 1804 (w)	1.43 (s, 15H, Cp*), −17.40 (s, 1H)
7	2036 (vs), 2005 (vs), 1961 (s), 1946 (m), 1933 (vs), 1716 (w), 1686 (w)	1.40 (s, 30 H, Cp*), −13.62 (t, 2H, J_{Rh-H} = 10 Hz)
8	2035 (vs), 1917 (vs, b)	1.36 (s, 15H, Cp*)
9	2060 (s), 2040 (vs), 1997 (vs)	1.76 (s, Cp*)
10	2019 (vs), 1907 (vs, b)	7.80−7.60 (bm, 4H, aryl), 7.06 (d, 4H, J_{H-H} = 8 Hz), 2.32 (s, 6H, Me), 1.54 (s, 15H, Cp*)
11	2012 (vs), 1905 (vs, b)	7.68 (d, 6H, J_{H-H} = 8 Hz), 7.05 (d, 6H, J_{H-H} = 8 Hz), 2.31 (s, 9H, Me), 1.54 (s, 15H, Cp*)

[a] The IR and NMR spectra were recorded at room temperature in heptane and C_6D_6, respectively, for compounds **4**−**7** and **9**. [b] The IR and NMR spectra were recorded in CH_2Cl_2 and $CDCl_3$, respectively, for compounds **8**, **10**, and **11**.

solvents were distilled from an appropriate drying agent under argon using Schlenk techniques or obtained from an Innovative Technology solvent purification system; when not in use, all distilled solvents were stored in Schlenk storage vessels equipped with high-vacuum Teflon stopcocks.[21] The photochemical studies were conducted with GE blacklight bulbs that had a maximum output at 366 ± 20 nm and a photon flux of ca. 1×10^{-6} einstein/min. Combustion analyses were performed by Atlantic Microlab, Norcross, GA.

All IR spectra were recorded on a Nicolet 6700 FT-IR spectrometer, using amalgamated NaCl cells capable of handling air-sensitive samples. The quoted ^1H NMR spectral data were recorded at either 200 or 500 MHz on Varian Gemini and Varian VXR-500 spectrometers, respectively, while the ^{13}C NMR spectra were recorded at 125 MHz on the latter spectrometer. The ESI-APCI mass spectra were recorded at the UC San Diego mass spectrometry facility in the positive ionization mode. Table 1 reports the IR and ^1H NMR spectral data for the new compounds **4**−**11**.

Synthesis of $H_2RhRe_2Cp^*(CO)_9$ (4), $HRh_2ReCp^*_2(CO)_6$ (5), and $HRhRe_3Cp^*(CO)_{14}$ (6) from $H_2Re_2(CO)_8$ (1) and $Cp^*Rh(CO)_2$ (2). In an argon-filled Schlenk tube was charged 50 mg (0.17 mmol) of **2** and 20 mL of hexane. The stirred solution was heated to reflux, after which 0.20 g (0.34 mmol) of **1** in 40 mL of hexane was added dropwise over the course of 30 min, followed by heating for an additional 1 h. TLC analysis of the cooled solution using CH_2Cl_2/hexane (3:7) as the eluent revealed the presence of one major spot belonging to cluster **4** (R_f = 0.53), along with minor spots belonging to clusters **5** (R_f = 0.21) and **6** (R_f = 0.45). The solvent was removed under vacuum and the residue purified by column chromatography over silica gel using the aforementioned mobile phase. Each product was recrystallized from hexane/benzene. Data for **4** are as follows: yield 96 mg (65% based on **2**); $^{13}C\{^1H\}$ NMR (CD_2Cl_2, 298 K): δ 181.99 (s, 2CO), 186.19 (d, J_{Rh-C} = 9.8 Hz); ESI-MS m/z fragmentation peaks at 558.76 $[Cp^*RhRe(CO)_4Na]^+$, 530.89 $[Cp^*RhRe(CO)_3Na]^+$, and 502.97 $[Cp^*RhRe(CO)_2Na]^+$. Anal. Calcd (found) for $C_{19}H_{17}O_9Re_2Rh$: C, 26.39 (26.41); H, 1.98 (1.95). Data for **5** are as follows: yield 11 mg (15% based on **2**); $^{13}C\{^1H\}$ NMR (CD_2Cl_2, 298 K): δ 186.86 (s, 1CO), 188.01 (s, 1CO), 189.11 (s, 2CO), 233.99 (dd, μ-CO, J_{Rh-C} = 32.4, 46.6 Hz), 234.01 (dd, μ-CO, J_{Rh-C} = 32.4, 46.6 Hz); ESI-MS m/z: 832.87 $[M + H]^+$. Data for **6** are as follows: yield 4.9 mg (2.4% based on **2**); ESI-MS: m/z fragmentation peaks at 558.76 $[Cp^*RhRe(CO)_4 + Na]^+$, 530.89 $[Cp^*RhRe(CO)_3 + Na]^+$, and 502.97 $[Cp^*RhRe(CO)_2 + Na]^+$.

Synthesis of $H_2RhRe_2Cp^*(CO)_9$ (4), $HRh_2ReCp^*_2(CO)_6$ (5), and $H_2Rh_2Re_2Cp^*_2(CO)_8$ (7) from 1 and $Cp^*_2Rh_2(CO)_2$ (3). To a small Schlenk flask under argon flush was added 60 mg (0.11 mmol) of $Cp^*_2Rh_2(CO)_2$ (**3**) and 73 mg (0.12 mmol) of **1**, after which 40 mL of hexane was added via syringe. The vessel was sealed against the atmosphere and heated at 55 °C in a thermostated bath for 2 h. TLC analysis using CH_2Cl_2/hexane (3:7) confirmed the presence of clusters **4** (major spot) and **5**, in addition to a new spot assigned to cluster **7** at R_f = 0.15. The three products were isolated by column chromatography and then recrystallized from hexane/benzene. Yield of **4**: 41 mg (39% based on **1**). Yield of **5**: 26 mg (28% based on **3**). Data for **7** are as follows: yield 11 mg (10% based on **3**); $^{13}C\{^1H\}$ NMR (CD_2Cl_2/2-MeTHF, 183 K) δ 187.56 (s, 6 CO), 232.02 (t, 2 μ-CO, J_{Rh-C} = 35 Hz); ESI-MS m/z 1096.65 $[M + Na]^+$ and 1074.66 $[M]^+$.

Synthesis of $Cp^*Rh(\mu\text{-}Cl)_3Re(CO)_3$ (8) from 4. A. Photochemical Reaction. A 30 mg sample (0.035 mmol) of **4** was dissolved in 5 mL of $CHCl_3$ and then irradiated at room temperature at 366 nm until TLC analysis signaled the complete consumption of **4**, which occurred after 15 h. The solution was filtered over a short plug of silica gel to remove the insoluble particulate matter present, albeit with some loss of product due to the irreversible binding of **8** to silica gel, and the solvent was then removed under vacuum. The crude residue was then recrystallized from CH_2Cl_2/hexane (1:1) to afford **8** as an orange solid in 12% yield (2.6 mg). Anal. Calcd (found) for $C_{13}H_{15}Cl_3O_3ReRh$: C, 25.40 (25.66); H, 2.46 (2.46).

B. Independent Thermolysis Reaction. Here 58 mg (0.094 mmol) of $[Cp^*RhCl_2]_2$ and 68 mg (0.19 mmol) of $ClRe(CO)_5$ were added to a medium Schlenk tube containing 50 mL of toluene under argon, after which the vessel was heated to 100 °C in a thermostated bath for 30 min. IR examination of the orange solution revealed the complete consumption of $ClRe(CO)_5$ and the presence of the desired product. The solvent was removed under reduced pressure, and the crude product was recrystallized as described above to afford 83 mg of **8** (72% yield).

Synthesis of $S_2Rh_3Cp^*(CO)_4$ (9) from the Reaction of 4 with H_2S. A Schlenk tube was charged with 30 mg (0.035 mmol) of **4** and 5 mL of benzene, after which the solution was saturated with H_2S for several minutes and the vessel sealed. The contents were heated at 55−60 °C for 18 h and then examined by TLC analysis, which revealed the presence of a single spot (R_f = 0.31 in 3:7 CH_2Cl_2/hexane) and extensive decomposition based on the large amount of material that remained at the origin of the plate. The sole spot was subsequently isolated by column chromatography and recrystallized from a mixture of hexane and benzene. Yield of orange **7**: 3.6 mg (50% based on rhodium). ESI-MS: m/z 642.46 $[M + Na]^+$ and 620.44 $[M + H]^+$.

Thermolysis Behavior of 4 in the Presence of *p*-Methylbenzenethiol and Synthesis of $Cp^*Rh(\mu\text{-}SC_6H_4Me\text{-}p)_3Re(CO)_3$ (11). To an argon-filled Schlenk tube was added 30 mg (0.035 mmol) of **4** and 10 mg (0.081 mmol) of *p*-methylbenzenethiol, followed by 5 mL of benzene via syringe. The vessel was sealed and then heated at 55 °C in a thermostated bath for 48 h, with TLC

(21) Shriver, D. F. *The Manipulation of Air-Sensitive Compounds*; McGraw-Hill: New York, 1969.

Table 2. X-ray Crystallographic Data and Processing Parameters for Clusters 4−7

compd	4	5	6	7
CCDC entry no.	710814	710813	710811	710812
cryst syst	monoclinic	orthorhombic	triclinic	triclinic
space group	$P2_1/n$	$Pna2_1$	$P\bar{1}$	$P\bar{1}$
a, Å	9.138(1)	17.617(3)	9.088(1)	11.2088(9)
b, Å	16.696(2)	14.817(2)	9.872(2)	16.790(1)
c, Å	15.210(2)	10.438(2)	16.810(3)	18.833(2)
α, deg			74.368(2)	115.067(3)
β, deg	98.965(2)		82.291(3)	105.305(3)
γ, deg			76.262(2)	90.396(3)
V, Å^3	2292.2(6)	2724.6(8)	1407.0(5)	3067.8(4)
mol formula	$C_{19}H_{17}O_9Re_2Rh$	$C_{26}H_{31}O_6ReRh_2$	$C_{24}H_{16}O_{14}Re_3Rh$	$C_{28}H_{32}O_8Re_2Rh_2$
fw	864.65	831.52	1189.87	1074.74
formula units per cell (Z)	4	4	2	2
D_{calcd} (Mg/m^3)	2.500	2.025	2.806	2.323
λ(Mo Kα), Å	0.710 73	0.710 73	0.710 73	0.710 73
μ (mm^{-1})	11.292	5.666	13.508	8.968
abs cor	empirical	semiempirical from equivalents	semiempirical from equivalents	semiempirical from equivalents
abs cor factor	1.0000/0.2557	0.180/0.130	0.6566/0.5402	0.068/0.039
total no. of rflns	19 298	57 888	6834	65 485
no. of indep rflns	5369	8511	6846	16 196
no. of data/res/params	5369/0/286	8511/1/326	6846/10/385	16 196/0/721
R1[a] ($I \geq 2\sigma(I)$)	0.0298	0.0193	0.0408	0.0651
wR2[b] (all data)	0.0511	0.0462	0.1227	0.1912
GOF on F^2	0.983	1.021	1.116	1.107
$\Delta\rho$(max), $\Delta\rho$(min) (e/Å^3)	1.035, −1.205	1.621, −0.718	3.182, −2.235	2.974, −2.745

[a] $R1 = \sum||F_o| - |F_c||/\sum|F_o|$. [b] $R2 = \{\sum[w(F_o^2 - F_c^2)^2]/\sum[w(F_o^2)^2]\}^{1/2}$.

analysis of the cooled solution revealing the presence of only compound **11** as a slow-moving orange spot at $R_f = 0.28$ (2:3 CH_2Cl_2/hexane). **11** was isolated by column chromatography over silica gel and then recrystallized from a 1:1 mixture of hexane and benzene. Yield of **11**: 5.6 mg (28%). ESI-MS: m/z 900.93 $[M + Na]^+$ and 754.95 $[M - SC_6H_4$-*p*-$Me]^+$.

Synthesis of Cp*Rh(μ-Cl)(μ-SC$_6$H$_4$Me-*p*)$_2$Re(CO)$_3$ (10) and 11 from 8 and *p*-Methylbenzenethiol. An alternative synthesis for **11** involves the use of the chloro-bridged dimer **8** and excess thiol. Here a toluene (50 mL) solution containing 0.10 g (0.16 mmol) of **8** and 0.10 g (0.81 mmol) of *p*-methylbenzenethiol were heated at reflux for 2 h under argon. TLC examination of the cooled solution using CH_2Cl_2/hexane (2:3) as the eluent revealed the presence of two spots assigned to **11** and **10** ($R_f = 0.16$), both of which were subsequently isolated by column chromatography. Yield of orange-red **10**: 58 mg (45%). ESI-MS for **10**: m/z 755.00 $[M - Cl^-]^+$. Yield of **11**: 43 mg (30%).

X-ray Structural Analyses. Single crystals of compounds **4**−**11** suitable for X-ray crystallography were grown from CH_2Cl_2 and hexane. The X-ray data for **4**, **9**, and **11**·$^1/_2$(hexane) (TCU) were collected on a a Bruker SMART 1000 CCD-based diffractometer at 213(2) K (**4**) and 233(2) K (**9** and **11**·$^1/_2$(hexane)), while the X-ray data for **5** and **7** (SDSU) were collected on a Bruker X8 APEX CCD diffractometer at 220(2) K. The frames were integrated with the available SAINT[22] software package using a narrow-frame algorithm, and the structures were solved and refined using the SHELXTL program package.[23] The X-ray data for compounds **6**, **8**, and **10** (UNT) were collected on an APEX II CCD-based diffractometer at 100(2) K, with the frames integrated with the available APEX2[24] software package using a narrow-frame algorithm and similarly applied refinement protocols. The molecular structures were checked by using PLATON,[25] and the non-hydrogen atoms were refined anisotropically. All hydrogen atoms were assigned calculated positions and allowed to ride on the attached carbon atom. The bridging hydride group(s) in clusters **4**−**7** were not located during refinement; the loci of these hydrides have been assigned on the basis of differences in the metal−metal bond lengths in each particular system, the arrangement of the ancillary CO groups about the cluster polyhedron, and VT NMR data. Tables 2 and 3 summarize the pertinent X-ray data and processing parameters for these compounds.

Kinetics Studies. The UV−vis studies employing **4** were conducted with a cluster concentration of ca. 10^{-4} M and used quartz UV−visible cells (1.0 cm width) that were equipped with a high-vacuum Teflon stopcock to facilitate handling on the vacuum line. For the reactions conducted under 1 atm of CO, CO was slowly bubbled through the stock solution containing **4** for several minutes prior to the start of the reaction. The experiment performed under high CO pressure was carried out in a carbon-steel 300 mL autoclave, with the internal CO pressure regulated with the aid of a Tescom pressure regulator. The autoclave was equipped with a tip tube that enabled sample removal for UV−vis analysis while maintaining constant CO pressure. The Hewlett-Packard 8452A diode array spectrometer employed in our studies was configured with a variable-temperature cell holder and was connected to a VWR constant-temperature circulator, allowing for the quoted temperatures to be maintained within ±0.5 K. The UV−vis kinetics were monitored by following the decrease of the 508 nm absorbance band of **4** as a function of time for at least 4−6 half-lives for all reactions other than the one reaction conducted at 34 atm of CO, which was examined out to 3 half-lives. The UV−vis derived rate constants quoted in Table 4 were determined by nonlinear regression analysis using the single-exponential function[26]

$$A(t) = A_\infty + \Delta A^* e^{-kt}$$

The activation parameters for the consumption of cluster **4** in the ligand decomposition study under CO were calculated from

(22) *Saint, Version 6.02*; Bruker Advanced Analytical X-ray Systems, Inc., Madison, WI, 1997−1999.

(23) *SHELXTL, Version 5.1*; Bruker Advanced Analytical X-ray Systems, Inc., Madison, WI, 1998.

(24) *APEX2 Version 2.14*; Bruker Advanced Analytical X-ray Systems, Inc., Madison, WI, 2007.

(25) Spek, A. L. *PLATON - A Multipurpose Crystallographic Tool*; Utrecht University, Utrecht, The Netherlands, 2006.

(26) The rate calculations were performed by using the commercially available program Origin6.0. Here the initial (A_0) and final (A_∞) absorbances and the rate constant were floated to give the quoted least-squares value for the first-order rate constant k.

Table 3. X-ray Crystallographic Data and Processing Parameters for Compounds 8−11

compd	**8**	**9**	**10**	**11**
CCDC entry no.	710809	710815	710810	710816
cryst syst	monoclinic	monoclinic	triclinic	triclinic
space group	$P2_1/n$	$P2_1/n$	$P\bar{1}$	$P\bar{1}$
a, Å	9.5709(6)	8.442(1)	10.0727(4)	10.085(1)
b, Å	14.737(9)	23.212(3)	11.3045(5)	12.184(1)
c, Å	12.0776(7)	10.236(1)	13.8148(9)	15.785(2)
α, deg			105.330(1)	75.129(2)
β, deg	90.189(1)	103.347(2)	105.702(1)	84.321(2)
γ, deg			105.900(1)	73.017(2)
V, Å^3	1703.6(2)	1951.7(4)	1355.6(1)	1792.3(3)
mol formula	$C_{13}H_{15}Cl_3O_3ReRh$	$C_{14}H_{15}O_4S_2Rh_3$	$C_{27}H_{29}ClO_3ReRhS_2$	$C_{34}H_{36}O_3ReRhS_3 \cdot {}^1/_2$(hexane)
fw	614.71	620.11	790.18	921.00
formula units per cell (Z)	4	4	2	2
D_{calcd} (Mg/m^3)	2.397	2.110	1.936	1.707
λ(Mo Kα), Å	0.710 73	0.710 73	0.710 73	0.710 73
μ (mm^{-1})	8.542	2.733	5.350	4.043
abs cor	semiempirical from equivalents	empirical	semiempirical from equivalents	empirical
abs cor factor	0.7600/0.3973	0.6747/0.5268	0.7871/0.4615	0.8701/0.7281
total no. of rflns	20 239	16 833	15 961	15 736
no. of indep rflns	3621	4553	5478	8191
no. od data/res/params	3621/0/195	4553/0/213	5478/0/323	8191/0/415
R1[a] ($I \geq 2\sigma(I)$)	0.0140	0.0510	0.0225	0.0522
wR2[b] (all data)	0.0311	0.0649	0.0474	0.1250
GOF on F^2	1.024	0.898	1.003	0.844
$\Delta\rho$(max), $\Delta\rho$(min) (e/Å^3)	0.655, −0.353	0.720, −0.775	0.890, −0.472	1.251, −1.035

[a] $R1 = \sum||F_o| - |F_c||/\sum|F_o|$. [b] $R2 = \{\sum[w(F_o^2 - F_c^2)^2]/\sum[w(F_o^2)^2]\}^{1/2}$.

Table 4. Experimental Rate Constants for the Thermolysis of Cluster 4 in the Presence of CO[a]

entry	temp (K)	solvent	ligand trap	10^5k (s^{-1})
1	325.5	toluene	CO, 1 atm	2.87 ± 0.03
2	333.0	toluene	CO, 1 atm	8.25 ± 0.01
3	333.0	heptane	CO, 1 atm	6.73 ± 0.01
4	333.0	2-MeTHF	CO, 1 atm	8.51 ± 0.02
5	333.0	CCl_4	CO, 1 atm	8.37 ± 0.05
6	333.0	toluene	CO, 34 atm	8.1 ± 0.9[b]
7	333.0	toluene	CO, 1 atm	8.29 ± 0.01[c]
8	333.0	toluene	CO, 1 atm	7.46 ± 0.04[d]
9	333.0	toluene	PPh_3	8.6 ± 0.1[e]
10	342.5	toluene	CO, 1 atm	22.2 ± 0.1
11	348.8	toluene	CO, 1 atm	41.3 ± 0.1
12	361.0	toluene	CO, 1 atm	150 ± 1

[a] The UV−vis kinetic data were collected in the specified solvent using a ca. 10^{-4} M solution of cluster **2** by following the decrease in the absorbance of the 508 nm band. [b] Reaction carried out in an autoclave at constant CO pressure. [c] Reaction carried out in the presence of 5 equiv of 9,10-dihydroanthracene. [d] Reaction carried out in the presence of 10 equiv of *p*-methoxyphenol. [e] Reaction carried out in the presence of 10 equiv of phosphine ligand.

a plot of $\ln(k/T)$ versus T^{-1},[27] with the error limits representing the deviation of the data points about the least-squares line of the Eyring plot.

Results and Discussion

I. Preparation, Spectroscopic Data, and Molecular Structures of Clusters 4−7. The new clusters **4**−**6** were obtained by following the general procedure outlined by Shapley in his synthesis of $H_2Re_2Ir(\eta^5\text{-ind})(CO)_9$.[11] Here the slow addition of a hexane solution of **1** to a refluxing hexane solution containing **2** eliminates the premature decomposition of **1**, which has limited stability at elevated temperature,[28] and allows for maximum conversion to the desired product **4**. TLC examination of the reaction solution after 90 min revealed the presence of **4** as the major product, in addition to two minor products assigned to clusters **5** and **6**. These products were isolated by column chromatography over silica gel as slightly air-sensitive solids. The three cluster products isolated from the reaction of **1** with **2** are depicted below.

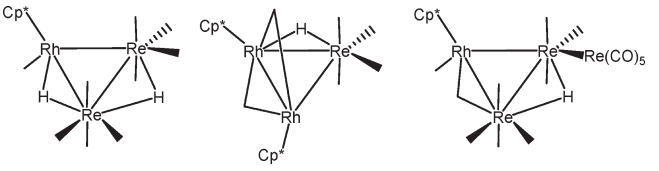

The IR and ^{1}H NMR spectroscopic data for **4** are reported in Table 1. **4** exhibits eight ν(CO) bands from 2100 to 1941 cm^{-1}, in agreement with the number of ν(CO) bands reported for $H_2Re_2Ir(\eta^5\text{-ind})(CO)_9$ and consistent with a cluster having only terminal carbonyl groups in solution. The ^{1}H NMR spectrum recorded in C_6D_6 at room temperature showed the expected Cp* singlet at δ 1.54, along with two edge-bridging hydrides centered at δ −15.96 and −16.04. The former hydride appears as a doublet (J_{Rh-H} = 26 Hz) and is consistent with a hydride that spans one of the Rh−Re bonds in the product, with the remaining hydride singlet at δ −16.04 readily assigned to the Re−Re bond in **4**. The magnitude of the J_{Rh-H} coupling constant matches those values reported for a series of $RhH(PPh_3)(SiR_3)X$ derivatives and several $PtRh_2$ clusters.[29,30] The locus of two hydrides in **4** is analogous to that formulated for the hydrides in the iridium derivative $H_2Re_2Ir(\eta^5\text{-ind})(CO)_9$.[11]

(27) Carpenter, B. K. *Determination of Organic Reaction Mechanisms*; Wiley-Interscience: New York, 1984.
(28) Masciocchi, N.; Sironi, A.; D'Alfonso, G. *J. Am. Chem. Soc.* **1990**, *112*, 9395.
(29) Haszeldine, R. N.; Parish, R. V.; Parry, D. J. *J. Chem. Soc. A* **1969**, 683.
(30) Green, M.; Mills, R. M.; Pain, G. N.; Stone, F. G. A.; Woodward P. *J. Chem. Soc., Dalton Trans.* **1982**, 1321.

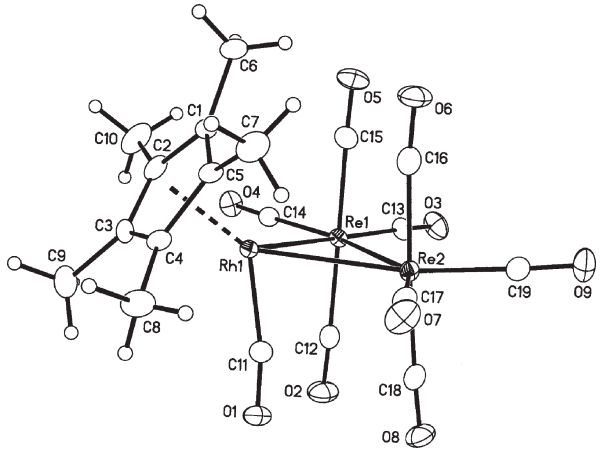

Figure 1. Thermal ellipsoid plot of the molecular structure of **4** showing the thermal ellipsoids at the 35% probability level. Selected bond distances (Å) and angles (deg): Re(1)−Rh(1) = 3.0140(5), Re(1)−Re(2) = 3.1202(4), Re(2)−Rh(1) = 2.8962(5), Cp*(centroid)−Rh(1)=1.896(2); Rh(1)−Re(1)−C(13) = 169.8(2), Rh(1)−Re(1)−C(14) = 100.2(2), Rh(1)−Re(2)−C(17) = 91.8(2), Rh(1)−Re(2)−C(19) = 170.9(2), Re(1)−Re(2)−C(19) = 116.6(2), Re(2)−Re(1)−C(13) = 114.1(2).

Examination of **4** by ESI mass spectrometry failed to yield a molecular ion for the cluster and instead gave *m*/*e* peaks for the sodiated fragmentation products $[Cp^*RhRe(CO)_n + Na]^+$ (where $n = 2-4$). The presence of a weak peak at *m*/*e* 1096.54 in the ESI mass spectrum is consistent with the tetrametallic species $[Cp^*_2Rh_2Re_2(CO)_8 + Na]^+$, whose origin may be traced to the dimerization of "$Cp^*RhRe(CO)_4$" fragments during residence in the electrospray ion source. The ability of the ESI MS technique to control aggregation states and direct the chemical syntheses of metastable organometallic compounds is a well-established phenomenon.[31]

Figure 1 shows the thermal ellipsoid plot of the molecular structure of **4**, which contains 48e and is electron precise in keeping with the tenets of polyhedral skeletal electron pair (PSEP) theory.[32] **4** exhibits a scalene $RhRe_2$ architecture, and the metal−metal bond distances range from 2.8962(5) Å (Re(2)−Rh(1)) to 3.1202(4) Å (Re(1)−Re(2)). Despite the fact that few structurally characterized $RhRe_2$ clusters exist, our data are in agreement with those Rh−Re and Re−Re bond distances in $RhRe_2(\mu\text{-}PPh_2)(CO)_{10}(PPh_3)$.[33,34] While the two hydrides were not located during data refinement, their locations are readily assigned to the Rh(1)−Re(1) and Re(1)−Re(2) vectors on the basis of hydride-induced structural trends found in $H_2Re_2Ir(\eta^5\text{-ind})(CO)_9$ and other polynuclear clusters.[11] Here the two hydrides are assumed to span the two longest metal−metal bonds, namely the Rh(1)−Re(1) and Re(1)−Re(2) vectors. The proposed sites for the two hydrides are further corroborated by the disposition of the ancillary CO groups about the cluster polyhedron. In triangular clusters, expanded M−M−CO angles significantly greater than the idealized value of ca. 90° serve as indicators for the location or proximity of an edge-bridging hydride.[35] The angles of 100.2(2)° (C(14)−Re(1)−Rh(1)), 114.1(2)° (C(13)−Re(1)−Re(2)), and 116.6(2)° (C(19)−Re(2)−Re(1)) reinforce our premise regarding the existence of bridging hydrides at the Rh(1)−Re(1) and Re(1)−Re(2) vectors in **4**. The observed angle of 60.5° that is formed by the planes containing the Cp* carbons and the three metal atoms confirms that the Cp* ligand is tipped significantly out of the metallic plane. The ancillary CO ligands are best viewed as terminal groups based on bond angles that range from 169.9(5)° (O(1)−C(11)−Rh(1)) to 178.6(5)° (O(7)−C(17)−Re(2)).

The effect of the Cp*Rh fragment on the fluxional properties of the CO groups in **4** was next explored by VT ^{13}C NMR spectroscopy. In the case of $H_2Re_2Ir(\eta^5\text{-ind})(CO)_9$, the ancillary CO groups do not exhibit any intrametallic scrambling, and the dynamic ^1H and ^{13}C behavior exhibited by the polyene and CO groups, respectively, was best explained by a hydride "jump" process involving the Ir−Re bound hydride.[11] Here the "jump" of the hydride between the two heterometallic bonds in $H_2Re_2Ir(\eta^5\text{-ind})(CO)_9$ is akin to the windshield wiper motion proposed for the equilibration of norbornyl cations.[36] The rapid pivoting of the iridium-anchored hydride between the two rhenium centers generates an effective mirror plane orthogonal to the metallic core and that bisects the Re−Re bond and polyene ligand.[37,38]

Samples of **4** used in the ^{13}C NMR studies (ca. 10−15% statistically enriched in ^{13}CO) were prepared from ^{13}CO-enriched samples of **1** or **2**. The use of either enriched starting material furnished ^{13}CO-enriched **4**. The room-temperature ^{13}C NMR spectrum of **4** in the carbonyl region exhibits two carbonyl resonances at δ 186.19 and 181.99 in a 7:2 integral ratio, with the former resonance appearing as a doublet due to coupling with rhodium ($J_{Rh-C} = 9.8$ Hz). A VT ^{13}C NMR study confirmed the fluxionality of the low-field resonance, which gradually broadened and coalescenced into the baseline by 183 K. Figure 2 shows selected ^{13}C NMR spectra for **4**, and these data provide support for a pairwise terminal−bridge−terminal exchange involving four CO groups through a plane coincident with the non-hydride-bridged Rh−Re vector, as outlined in Scheme 2. Here the rapid averaging of seven CO groups across the two vertical Rh−Re planes (red and blue paths) readily accounts for the observed

(31) Neo, K. E.; Huynh, H. V.; Koh, L. L.; Henderson, W.; Hor, T. S. A. *J. Organomet. Chem.* **2008**, *693*, 1628.

(32) Mingos, D. M. P.; Wales, D. J. *Introduction to Cluster Chemistry*; Prentice Hall: Englewood Cliffs, NJ, 1990.

(33) Haupt, H.-J.; Flörke, U.; Beckers, H.-G. *Inorg. Chem.* **1994**, *33*, 3481.

(34) For trinuclear $RhRe_2$ compounds possessing metal−metal bond distances similar to those values exhibited by **4**, see: (a) Bruce, M. I.; Low, P. J.; Skelton, B. W.; White, A. H. *J. Chem. Soc., Dalton Trans.* **1993**, 3145. (b) Beckers, H.-G.; Flörke, U.; Haupt, H.-J. *Angew. Chem., Int. Ed.* **1995**, *34*, 1325. (c) Haupt, H.-J.; Wittbecker, R.; Haferkamp, P.; Flörke, U. *Z. Anorg. Allg. Chem.* **2001**, *627*, 2359.

(35) (a) Churchill, M. R.; Hollander, F. J.; Lashewycz, R. A.; Pearson, G. A.; Shapley, J. R. *J. Am. Chem. Soc.* **1981**, *103*, 2430. (b) Churchill, M. R.; Hollander, F. J. *Inorg. Chem.* **1981**, *20*, 4124.

(36) For a general discussion on the reactivity and spectroscopic properties of nonclassical carbocations, see: March, J. *Advanced Organic Chemistry*, 4th ed.; Wiley: New York, 1992.

(37) The hydride "jump" process was initially invoked to account for the fluxional behavior of the CO ligands in the heterometallic cluster $H_2Re_2Pt(CO)_8(cod)$.[12e]

(38) For hydride fluxionality in other trimetallic clusters, see: (a) Bracker-Novak, J.; Hajela, S.; Lord, M.; Zhang, M.; Rosenberg, E.; Gobetto, R.; Milone, L.; Osella, D. *Organometallics* **1990**, *9*, 1379. (b) Day, M.; Espitia, D.; Hardcastle, K. I.; Kabir, S. E.; Rosenberg, E.; Gobetto, R.; Milone, L.; Osella, D. *Organometallics* **1991**, *10*, 3550. (c) Day, M.; Freeman, W.; Hardcastle, K. I.; Isomaki, M.; Kabir, S. E.; McPhillips, T.; Rosenberg, E.; Scott, L. C.; Wolf, E. *Organometallics* **1992**, *11*, 3376. (d) Aime, S.; Dastrú, W.; Gobetto, R.; Arce, A. J. *Organometallics* **1994**, *13*, 3737. (e) Gobetto, R.; Hardcastle, K. I.; Kabir, S. E.; Milone, L.; Nishimura, N.; Botta, M.; Rosenberg, E.; Yin, M. *Organonetallics* **1995**, *14*, 3068. (f) Deeming, A. J.; Hassan, M. M.; Kabir, S. E.; Nordlander, E.; Tocher, D. A. *Dalton Trans.* **2004**, 3709.

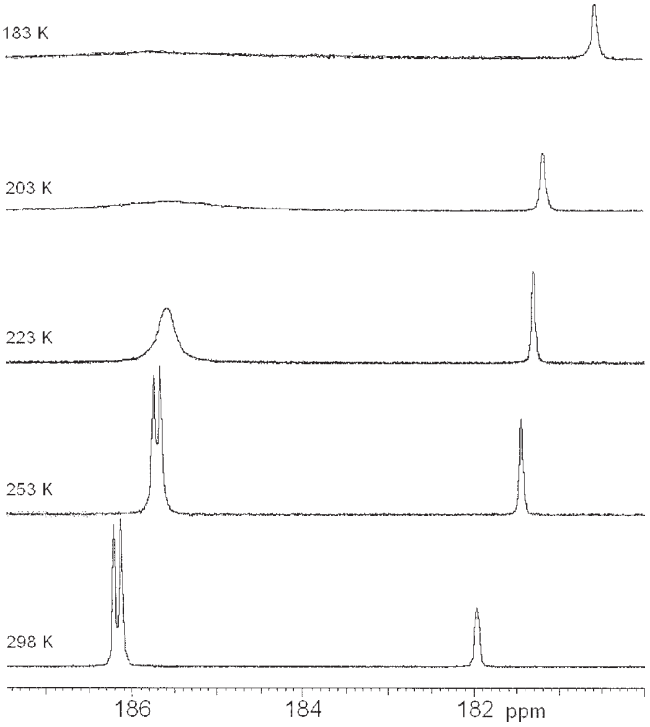

Figure 2. VT ^{13}C NMR spectra of ^{13}CO-enriched **4** in CD_2Cl_2-d_2/2-MeTHF from 298 to 183 K.

doublet at δ 186.19 at room temperature. The magnitude of the weighted-average $^1J_{Rh-C}$ value measured for the doublet is in excellent agreement with the ca. 70 Hz coupling reported for terminally bound CO ligands in a diverse group of di- and polynuclear rhodium carbonyl compounds.[39] The two CO groups in Scheme 2 labeled as e and e′ are perpendicular to their respective RhRe exchange plane and should appear as separate one-carbon resonances in the absence of accidental degeneracy, especially if the hydride associated with the Rh−Re vector is static. However, if a rapid hydride jump is operational, as in the case of $H_2Re_2Ir(\eta^5\text{-ind})(CO)_9$, these two distinct CO groups would be rendered equivalent through the time-averaging motion of the hydride about both Rh−Re bonds. That this particular hydride is fluxional is supported by its relative temperature invariance, as verified by the VT ^{1}H NMR profiles deposited as Supporting Information. We would add that the ^{13}C NMR features displayed by **4** closely parallel those data reported for the isobal mixed-metal clusters $RhOs_2(\eta^5\text{-}C_5R_5)(CO)_9$ (where

Scheme 2

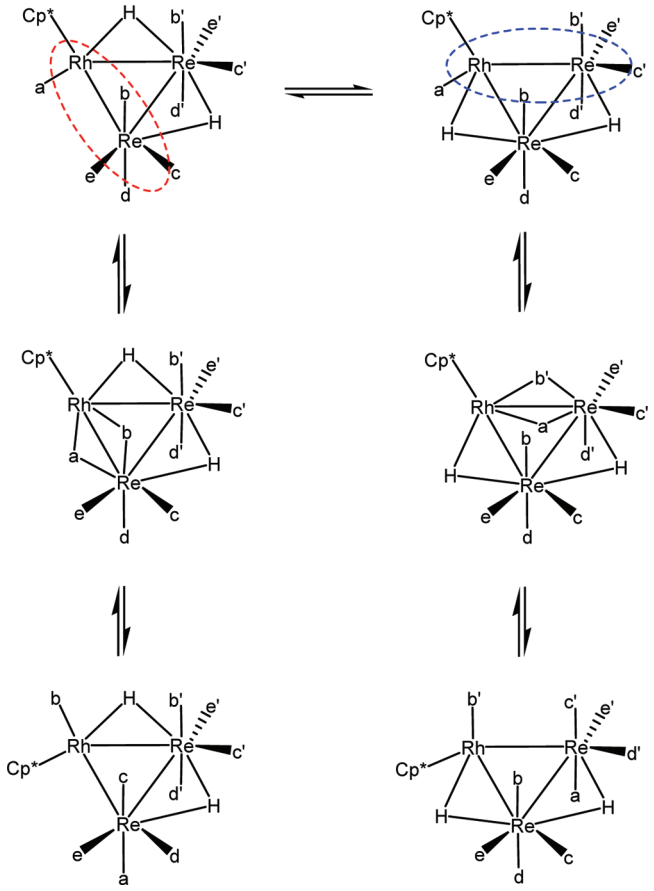

R = H, Me).[40−42] Takats has shown that the more electron rich Cp* ligand actually lowers the energy barrier for the in-plane CO exchange about the Rh−Os vectors, and this phenomenologically established effect likely serves as the basis for the change in the dynamic CO behavior in **4** vis-à-vis $H_2Re_2Ir(\eta^5\text{-ind})(CO)_9$.

Accompanying the formation of **4** are the cluster compounds **5** and **6**. These minor products were readily isolated by careful column chromatography over silica gel, and they were fully characterized by traditional spectroscopic and crystallographic methods. **5** and **6** were formed in yields of 15% and ca. 2%, respectively. The thermal ellipsoid plot of the molecular structure of **5** is shown in Figure 3, where the presence of a triangular Rh_2Re core is confirmed. The bridging hydride was not located during refinement, but its presence was ascertained by ^{1}H NMR spectroscopy. Cluster **5** contains 48e and is isolobal with **4**. The Rh−Rh bond distance of 2.6675(4) Å in **5** compares favorably with those Rh−Rh bond lengths reported for the mixed-metal clusters $MoRh_2Cp^*_2(CO)_8$, $Rh_4PtCp^*_4(CO)_4$, and $Rh_2PtCp^*_2(CO)_3(PPh_3)$.[43] The Rh(2)−Re(1) bond distance of 2.9513(4) Å is ca. 0.06 Å longer than the Rh(1)−Re(1) vector (2.8817(4) Å), with the slight elongation attributed to the hydride ligand that spans the former heterometal bond. The observed 122.8(1)° bond angle for the C(23)−Re(1)−Rh(2)

(39) (a) Cotton, F, A.; Kruczynski, L.; Shapiro, B. L.; Johnson, L. F. *J. Am. Chem. Soc.* **1972**, *94*, 6191. (b) Evans, J.; Johnson, B. F. G.; Lewis, J.; Norton, J. R. *J. Chem. Soc., Chem. Commun.* **1973**, 807. (c) Aldridge, M. L.; Green, M.; Howard, J. A. K.; Pain, G. N.; Porter, S. J.; Stone, F. G. A.; Woodard, P. I. *J. Chem. Soc., Dalton Trans.* **1982**, 1333. (d) Heaton, B. T.; Pergola, R. D.; Strona, L.; Smith, D. O. *J. Chem. Soc., Dalton Trans.* **1982**, 2553. (e) Fumagalli, A.; Martinengo, S.; Chini, P.; Galli, D.; Heaton, B. T.; Pergola, R. D. *Inorg. Chem.* **1984**, *23*, 2947. (f) Fumagalli, A.; Martinengo, S.; Ciani, G.; Moret, M.; Sironi, A. *Inorg. Chem.* **1992**, *31*, 2900.

(40) For treatises on the isolobal theory, see: (a) Hoffmann, R. *Angew. Chem., Int. Ed.* **1982**, *21*, 711. (b) Stone, F. G. A. *Angew. Chem., Int. Ed.* **1984**, *23*, 89. (c) Albright, T. A.; Burdett, J. K.; Whangbo, M. H. *Orbital Interactions in Chemistry*; Wiley-Interscience: New York, 1985.

(41) (a) Hsu, L.-Y.; Hsu, W.-L.; Jan, D.-Y.; Marshall, A. G.; Shore, S. G. *Organometallics* **1984**, *3*, 591. (b) Washington, J.; Takats, J. *Organometallics* **1990**, *9*, 925. (c) Cooke, J.; Takats, J. *Organometallics* **1995**, *14*, 698.

(42) For related in-plane migrations of CO in phosphite-substituted Os_3 clusters, see: Alex, R. F.; Pomeroy, R. K. *Organometallics* **1987**, *6*, 2437.

(43) (a) Green, M.; Howard, J. A. K.; Mills, R. M.; Pain, G. N.; Stone, F. G. A.; Woodward, P. *J. Chem. Soc., Chem. Commun.* **1981**, 869. (b) Green, M.; Howard, J. A. K.; Pain, G. N.; Stone, F. G. A. *J. Chem. Soc., Dalton Trans.* **1982**, 1327. (c) Barr, R. D.; Green, M.; Howard, J. A. K.; Marder, T. B.; Orpen, A. G.; Stone, F. G. A. *J. Chem. Soc., Dalton Trans.* **1984**, 2757.

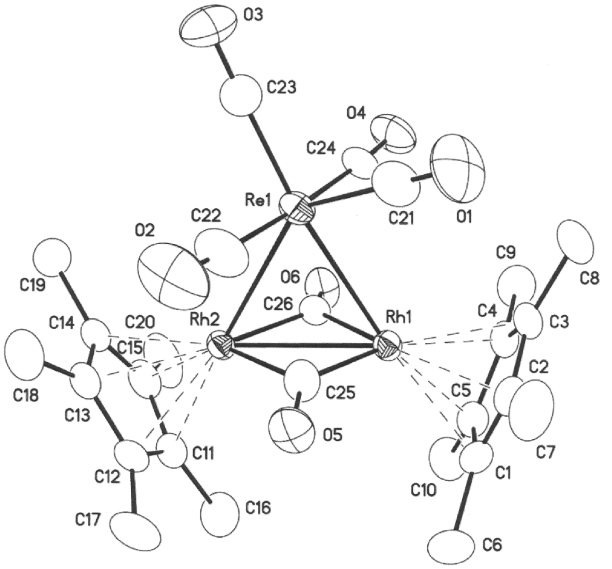

Figure 3. Thermal ellipsoid plot of the molecular structure of **5** showing the thermal ellipsoids at the 50% probability level. Selected bond distances (Å) and angles (deg): Re(1)−Rh(1) = 2.8817(4), Re(1)−Rh(2) = 2.9513(4), Rh(1)−Rh(2) = 2.6675(4), Cp*(centroid)−Rh(1)=1.894(1), Cp*(centroid)−Rh(2)=1.869(1), Rh(1)−C(26) = 1.974(3), Rh(1)−C(25) = 1.926(3), Rh(2)−C(25) = 2.107(3), Rh(2)−C(26) = 2.005(3); Rh(1)−Re(1)−C(21) = 92.3(1), Rh(2)−Re(1)−C(23) = 122.8(1).

atoms is consistent with the proposed location of the hydride ligand. The terminal CO groups on the Re(1) center are staggered slightly relative to the plane defined by the three metals and display an orientation with respect to the Cp*Rh-(μ-CO)$_2$RhCp* moiety, much like the disposition displayed by the Mo(CO)$_5$ fragment in MoRh$_2$Cp*$_2$(CO)$_8$,[43c] albeit less pronounced in the case of **5**. This is reasonable given the isolobal relationship between the two different edge-bridging Mo(CO)$_5$ and HRe(CO)$_4$ fragments.[44] The IR spectrum of **5** exhibits three terminal carbonyl stretching bands at 2057 (s), 1968 (vs), and 1936 (s) cm^{-1}, along with a lower energy bridging ν(CO) band at 1804 (m) cm^{-1} consistent with the presence of the Cp*Rh(μ-CO)$_2$RhCp* moiety. The ^{1}H NMR spectrum displays a Cp* singlet at δ 1.84 and a high-field doublet at δ −18.45 in a 30:1 ratio. The hydride resonance appears as a doublet (^1J = 32 Hz) due to its coupling to a single rhodium atom. This splitting is important because it indicates that the observed singlet for the inequivalent Cp* groups does not derive from a fluxional process that time-averages both Cp*Rh moieties about the Re−H bond, as reported by Stone for the cationic cluster [HRh$_2$PtCp*$_2$-(CO)$_4$]$^+$ and its phosphine-substituted derivatives.[43a,b] Since the rapid rotation of the Cp*Rh(μ-CO)$_2$RhCp* moiety about the Rh−H bond in **5** would afford a triplet pattern for the hydride, we can conclude that the two Cp* moieties are accidentally degenerate in C$_6$D$_6$. The room-temperature ^{13}C NMR spectrum of ^{13}CO-enriched **5** displays three terminal carbonyl groups at 186.86, 188.01, and 189.11 in an integral ratio of 1:1:2, respectively, for the Re(CO)$_4$ moiety, with the two bridging CO groups associated with

(44) The Mo(CO)$_5$ and HRe(CO)$_4$ fragments are well-known carbene equivalents based on their d^6-ML$_5$ and d^8-ML$_4$ designations, respectively. The HRe(CO)$_4$ fragment may also be viewed within the context of the corresponding carbonylmetalate anion Re(CO)$_4^-$, whose protonation does not alter its frontier orbital properties.[40]

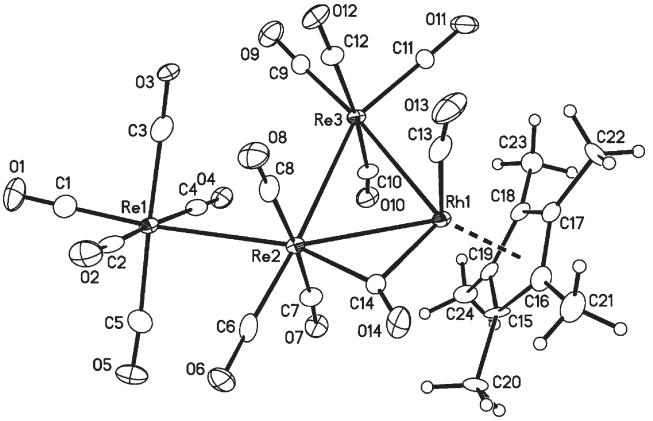

Figure 4. Thermal ellipsoid plot of the molecular structure of **6** showing the thermal ellipsoids at the 50% probability level. Selected bond distances (Å) and angles (deg): Re(1)−Re(2) = 3.0480(8), Re(2)−Re(3) = 3.1142(7), Re(2)−Rh(1) = 2.913(1), Re(3)−Rh(1) = 2.861(1), Re(2)−C(14) = 2.00(1), Rh(1)−C-(14) = 2.18(1), Cp*(centroid)−Rh(1) = 1.917(1); Re(1)−Re-(2)−Re(3) = 100.11(2), C(9)−Re(3)−Re(2) = 118.4(3), C(11)−Re(3)−Rh(1) = 96.4(3).

the Cp*Rh moieties appearing as two closely spaced sets of doublet of doublets centered at δ 233.99 and 234.01. Finally, the ESI mass spectrum revealed a prominent peak at m/e 832.87 attributed to the molecular ion for [**5** + H]$^+$.

The isolation of **6** proved to be problematic, because it readily decomposed during chromatography. **6** was also found to be mildly light- and temperature-sensitive, with noticeable decomposition to cluster **4** observed when solutions of **6** were monitored by TLC, IR, and NMR analyses. The ^{1}H NMR spectrum of **6** exhibits two singlets at δ 1.43 and −17.40 in a 15:1 integral ratio that are attributed to Cp* and hydride groups, respectively. The observed hydride singlet indicates that hydride does not span one of the Rh−Re vectors in **6**. The ESI mass spectrum recorded for **6** matched that of **4** exactly with peaks at m/z 558.80, 530.89, and 503.06 for the formation of the sodiated fragmentation products [Cp*RhRe(CO)$_n$ + Na]$^+$ (where n = 2−4). Unlike **4**, no higher order dimer-based fragmentation peaks were observed for **6**. The molecular structure of **6**, which was established by X-ray diffraction analysis, consists of a spiked triangular array of metals. Figure 4 shows the thermal ellipsoid plot of the molecular structure of **6**, where the pendant or spiked Re(CO)$_5$ moiety is confirmed. While the necessary hydride ligand was not located during crystallographic refinement, its presence was ascertained by ^{1}H NMR spectroscopy (vide supra). **6** contains 64e, in agreement with PSEP theory, and its geometry is similar to that of other spiked triangular motifs.[45] Of the 14 carbonyl groups in **6**, thirteen are terminal and one is bridging; the bond

(45) (a) Wang, S. R.; Wang, S.-L.; Cheng, C. P.; Yang, C. S. *J. Organomet. Chem.* **1992**, *431*, 215. (b) Housecroft, C. E.; Humphrey, J. S.; Keep, A. K.; Matthews, D. M.; Seed, N. J.; Haggerty, B. S.; Rheingold, A. L. *Organometallics* **1992**, *11*, 4048. (c) Beringhelli, T.; D'Alfonso, G.; Zarini, M. *J. Chem. Soc., Dalton Trans.* **1995**, 2407. (d) Bergamo, M.; Beringhelli, T.; D'Alfonso; Ciani, G.; Moret, M.; Sironi, A. *Organometallics* **1996**, *15*, 1637. (e) Ang, H. G.; Koh, L. L.; Ang, S.; Ng, S. Y.; Yang, G. Y. *J. Chem. Soc., Dalton Trans.* **1996**, 4083. (f) Bergamo, M.; Beringhelli, T.; Ciani, G.; D'Alfonso, G.; Moret, M.; Sironi, A. *Inorg. Chim. Acta* **1997**, *259*, 291. (g) Cabeza, J. A.; Moreno, M.; Riera, V.; Rosales-Hoz, M. D. J. *Inorg. Chem. Commun.* **2001**, *4*, 57. (h) Wong, W.-Y.; Ting, F.-L.; Lam, W.-L. *Eur. J. Inorg. Chem.* **2001**, 623. (i) Panigati, M.; Donghi, D.; D'Alfonso, G.; Mercandelli, P.; Sironi, A.; D'Alfonso, L. *Inorg. Chem.* **2006**, *45*, 10909.

distances and angles exhibited by these ligands fall within acceptable ranges reported for such CO groups.[46] The heterometallic Rh(1)−Re(2) and Rh(1)−Re(3) bonds exhibit distances of 2.913(1) and 2.861(1) Å, respectively, with the latter bond bridged by the C(14)O(14) moiety. The 3.0480(8) Å (Re(1)−Re(2)) bond length associated with the spiked $Re(CO)_5$ moiety is similar to that Re−Re bond distance of 3.041(1) Å reported for $Re_2(CO)_{10}$, and this feature suggests that this spiked Re(1)−Re(2) bond does not serve as a locus for the hydride ligand.[47] The location of the bridging hydride in **6** may be confidently assigned to the Re(2)−Re(3) vector on the basis of its elongated bond distance relative to the Re(1)−Re(2) vector and the stereochemical disposition of the ancillary CO groups about the Re(2) and Re(3) centers. The Re(2)−Re(3) bond length of 3.1142(7) Å and bond angles of 118.4(3) and 100.1(2)° for the C(9)−Re(3)−Re(2) and Re(1)−Re(2)−Re(3) linkages, respectively, strongly support an equatorially bound hydride ligand.[35]

An alternative synthesis of **4** using the unsaturated dimers **1** and **3** was also investigated. The latter dimer, which functions as a source of the Cp*Rh(CO) fragment, has been employed as a starting material for the construction of numerous rhodium-containing mixed-metal clusters.[48] Refluxing an equimolar mixture of **1** and **3** in hexane furnished clusters **4** and **5** in yields of 39% and 28%, respectively, in addition to a new species identified as **7** in 10% yield. The IR spectrum of **7** exhibits five distinct terminal carbonyl groups from 2036 to 1933 cm^{-1}, along with two lower energy ν(CO) bands at 1716 and 1686 cm^{-1} that indicate the presence of face-capping CO groups. The composition of **7**, and with it the two hydride ligands that were not located during the structural refinement (vide infra), are supported by ESI mass spectrometry on the basis of peaks at *m*/*e* 1074.66 and 1096.65 attributed to $[M]^+$ and the sodiated pseudomolecular ion $[M + Na]^+$, respectively.

The room-temperature ^{1}H NMR spectrum of **7** in C_6D_6 exhibits resonances at δ 1.40 (30 H) and −13.62 (2 H) for the Cp* and hydride groups, with the latter appearing as a hydride triplet (J_{Rh-H} = 10 Hz) due to coupling to both rhodium atoms. The dynamic behavior of these hydrides was subsequently established by VT NMR spectroscopy in CD_2Cl_2. Lowering the temperature to −70 °C led to the collapse of the hydride triplet and formation of a doublet centered at δ −14.16 (J_{Rh-H} = 20 Hz), as illustrated in Figure 5.[49] The slow-exchange NMR data support the existence of either edge-bridging (Rh−Re) or face-capping ($RhRe_2$) hydrides. Transformation of the doublet into a triplet as the temperature is raised is consistent with a rapid exchange of the hydrides about the cluster polyhedron to afford hydrides that bridge a RhRe vector or cap the two Rh_2Re faces in **7**. The fact that the magnitude of the rhodium−hydride coupling at room temperature is half that observed at low temperature is strong evidence for rapid hydride migration about the cluster polyhedron and hydride association with both rhodium atoms.[50,51]

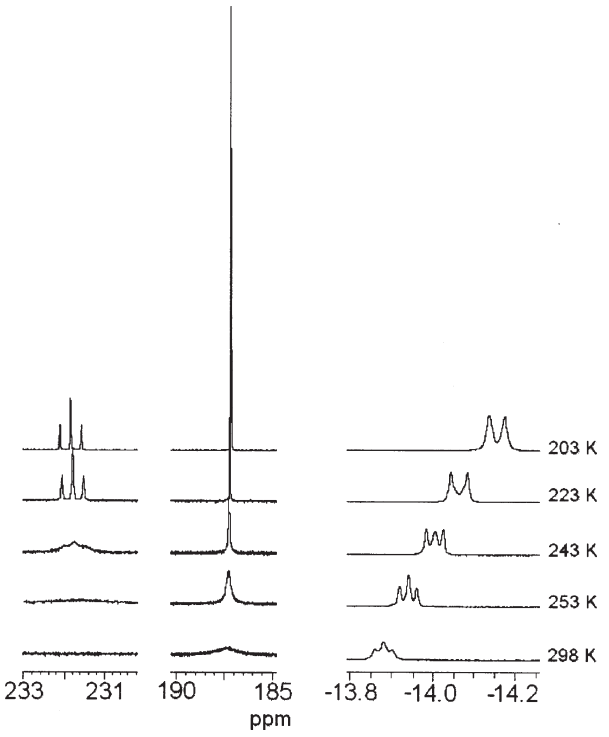

Figure 5. ^{1}H (right) and ^{13}C (left) VT NMR of **7** in CD_2Cl_2 from 298 to 203 K. The pertinent terminal and bridging carbonyl regions are depicted separately, and the spectra have been recorded using ^{13}CO-enriched **7**.

Figure 5 depicts selected VT ^{13}C NMR spectra of **7**. The broad resonance observed at ca. δ 188 at room temperature is readily ascribed to the terminal CO groups of the $Re(CO)_3$ moieties, while the two CO groups associated with the rhodium atoms are not discernible. Lowering the temperature to 203 K leads to a sharpening of the high-field terminal carbonyl resonance and the appearance of a triplet at δ 232.02 ($^1J_{Rh-C}$ = 35 Hz) assignable to the bridging CO groups that span the Rh−Rh vector. At 203 K the carbonyl resonances at δ 232.02 and 187.56 display an integral ratio of 1:3, respectively, in agreement with formulated structure. The carbonyl singlet exhibited by the $Re(CO)_3$ moieties is consistent with a rapid, localized CO exchange at each $Re(CO)_3$ unit similar to that behavior reported for

(46) (a) Orpen, A. G.; Brammer, L.; Allen, F. H.; Kennard, O.; Watson, D. G.; Taylor, R. *J. Chem. Soc., Dalton Trans.* **1989**, S1. (b) Horwitz, C. P.; Shriver, D. F. *Adv. Organomet. Chem.* **1984**, *23*, 219.

(47) Churchill, M. R.; Amoh, K. N.; Wasserman, H. J. *Inorg. Chem.* **1981**, *20*, 1609.

(48) (a) Green, M.; Jeffery, J. C.; Porter, S. J.; Razay, H.; Stone, F. G. A. *J. Chem. Soc., Dalton Trans.* **1982**, 2474. (b) Farrugia, L. J.; Orpen, A. G.; Stone, F. G. A. *Polyhedron* **1983**, *2*, 171. (c) Jeffery, J. C.; Marsden, C.; Stone, F. G. A. *J. Chem. Soc., Dalton Trans.* **1985**, 1315. (d) Jan, D.-Y.; Hsu, L.-Y.; Hsu, W.-L.; Shore, S. G. *Organometallics* **1987**, *6*, 274. (e) Lindsell, W. E.; McCullough, K. J. *J. Organomet. Chem.* **1988**, *346*, 425. (f) Barnes, C. E.; Dial, M. R.; Orvis, J. A.; Staley, D. L.; Rheingold, A. L. *Organometallics* **1990**, *9*, 1021. (g) Jeffery, J. C.; Jellis, P. A.; Rudd, G. E. A.; Sakanishi, S.; Stone, F. G. A.; Whitehead, J. *J. Organomet. Chem.* **1999**, *582*, 90.

(49) The ^{1}H NMR spectrum of **7** recorded in CD_2Cl_2 at room temperature exhibits singlet and triplet resonances at δ 1.55 (30H, Cp* groups) and −13.88 (2H, J_{Rh-H} = 20 Hz).

(50) (a) The observed ^{1}H triplet resonance in cluster **7** in the fast-exchange regime is consistent with either face-capping hydrides (i.e., hydrides that cap Rh_2Re polyhedral faces) or edge-bridging hydrides that span Rh−Re vectors. In the case of the latter scenario, the resulting AA′XX′ spin system would furnish a hydride triplet in the ^{1}H NMR spectrum when $J_{AX} = J_{AX'}$. (b) Bovey, F. A. *Nuclear Magnetic Resonance Spectroscopy*; Academic Press: New York, 1969.

(51) For structural and dynamical studies involving face-capping hydride ligands, see: (a) Huie, B. T.; Knobler, C. B.; Kaesz, H. D. *J. Am. Chem. Soc.* **1978**, *100*, 3059. (b) Green, M.; Mead, K. A.; Mills, R. M.; Salter, I. D.; Stone, F. G. A.; Woodward, P. *J. Chem. Soc., Chem. Commun.* **1982**, 51. (c) Fryzuk, M. D. *Organometallics* **1982**, *1*, 408. (d) Ricci, J. S.; Koetzle, T. F.; Goodfellow, R. J.; Espinet, P.; Maitlis, P. M. *Inorg. Chem.* **1984**, *23*, 1828. (e) Lin, R.-C.; Chi, Y.; Peng, S.-M.; Lee, G.-H. *Inorg. Chem.* **1992**, *31*, 3818. (f) Bau, R.; Ho, N. N.; Schneider, J. J.; Mason, S. A.; McIntyre, G. J. *Inorg. Chem.* **2004**, *43*, 555.

$[H_3Re_3(CO)_{10}]^{2-}$, $[HRe_6C(CO)_{18}(AuPPh_3)_2]^-$, and numerous clusters with $M(CO)_3$ vertices.[52−54] The chemical shift of the terminal and bridging CO groups is unaffected by temperature, and this rules out an intramolecular exchange of CO groups between the different metals in **7**. The observed temperature-dependent broadening of the CO resonances is consistent with scalar coupling of the CO groups with the ^{185,187}Re ($I = {}^5/_2$) isotopomers.[55]

7 crystallizes as two independent molecules in the unit cell that reveal no significant differences. Figure 6 shows the thermal ellipsoid plot of the molecular structure of one of the molecules of **7** and confirms the presence of a Rh_2Re_2 tetrahedral core. As mentioned earlier, the ancillary hydrides were not crystallographically located, but their inclusion is necessary to achieve an electron count of 60e consistent with PSEP theory and compliance with the ^{1}H NMR data. To our knowledge, **7** represents the first structurally characterized Rh_2Re_2 cluster. The 2.717(1) Å bond distance exhibited by the Rh(1)−Rh(2) vector is similar to the Rh−Rh distance reported for the related tetrahedral clusters $Rh_2Ir_2Cp^*_2(CO)_7$, $Rh_2M_2Cp^*_2(CO)_8$ (where M = Ru, Os), and $Rh_2Mo_2Cp^*_2Cp_2(CO)_4$ that contain Cp*Rh moieties.[48b,d,e,56] The four Rh−Re bond distances range from 2.884(1) Å (Rh(1)−Re(1)) to 2.935(1) Å (Rh(2)−Re(1)), and the mean distance of 2.908 Å compares well to the non-hydride-bridged Rh−Re bond length in both **4** and **5** and the non-carbonyl-bridged Rh−Re vector in **6**. The Re(1)−Re(2) bond distance of 2.8482(8) Å is significantly shorter than the Re−Re bond distance of 3.041(1) Å reported for $Re_2(CO)_{10}$ and the Re−Re bond distances that are well in excess of 3.200 Å in $H_3Re_3(CO)_{12-n}(MeCN)_n$ (where $n = 0, 1, 3$)[57] and the Re−Re bond distances found in clusters **4** and **6**.[45] In fact, the Re(1)−Re(2) bond distance in **7** is in close agreement with those Re−Re distances found in the face-capped clusters $[H_3Re_3(CO)_9(\mu_3\text{-}AuPPh_3)]^-$ and $HRe_3(CO)_6(\mu_3\text{-}Cl)(\mu\text{-}PPh_2)_3$.[58] The Rh(1)Rh(2)Re(1) and Rh(1)Rh(2)Re(2) faces are each capped by a single carbonyl group in a highly asymmetric fashion. The Rh−C bond distances associated with the face-capping C(27)O(7) and C(28)O(8) groups range from 1.99(1) Å (Rh(1)−C(28))] to 2.17(1) Å (Rh(2)−C(28)) and are significantly shorter than their counterpart Re−C bond distances of 2.40(2) Å (Re(1)−C(27)) and 2.35(2) Å (Re(2)−C(28)). The bond-length distortions found in the two μ_3-CO groups mimic the behavior of those face-capping CO ligands in the bis(Cp*Rh)-substituted clusters $Rh_2Ru_2Cp^*_2(CO)_8$ and $Rh_2Mo_2Cp^*_2Cp_2(CO)_4$.[48e,56,59]

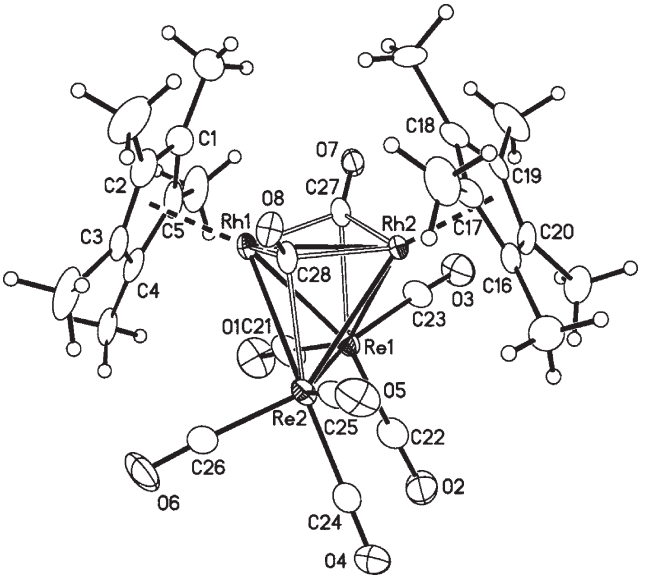

Figure 6. Molecular structure of one of the two independent molecules of **7** in the unit cell, showing thermal ellipsoids at the 50% probability level. Selected bond distances (Å) and angles (deg): Rh(1)−Rh(2) = 2.717(1), Rh(1)−Re(1) = 2.884(1), Rh(1)−Re(2) = 2.888(1), Rh(2)−Re(2) = 2.924(1), Rh(2)−Re(1) = 2.935(1), Re(2)−Re(1) = 2.8482(8), Cp*(centroid)−Rh(1) = 1.898(1), Cp*(centroid)−Rh(2) = 1.879(1), Rh(1)−C(28) = 1.99(1), Rh(1)−C(27) = 2.00(1), Rh(2)−C(27) = 2.08(1), Rh(2)−C(28) = 2.17(1), Re(1)−C(27) = 2.40(2), Re(2)−C(28) = 2.35(2); C(22)−Re(1)−Re(2) = 96.1(6), C(21)−Re(1)−Re(2) = 124.8(6), C(23)−Re(1)−Re(2) = 146.6(6), C(24)−Re(2)−Re(1) = 94.4(6), C(25)−Re(2)−Re(1) = 144.4(5), C(26)−Re(2)−Re(1) = 127.3(5).

II. Decomposition Kinetics of 4 in the Presence of CO. The stability of **4** under CO was investigated, given the reports of PPh_3-induced decomposition of $H_2Re_2Ir(\eta^5\text{-ind})(CO)_9$ and the limited stability of the trinuclear clusters $Ir_{3-x}Rh_x(\eta^5\text{-ind})_3(CO)_3$ (where $x = 0-3$) under CO.[11,60] The latter clusters react rapidly with added CO at room temperature to afford the corresponding mononuclear compound(s) $M(\eta^5\text{-ind})(CO)_2$. The lability of **4** was initially probed by stirring a heptane solution of **4** under ^{13}CO (1 atm) for a period of 24 h. IR spectroscopy verified the absence of ^{13}CO incorporation into cluster **4**, and this allows us to rule out the formation of a significant concentration of unsaturated cluster from a manifold derived by either CO or H_2 loss at room temperature. **4** is thermally sensitive and decomposes under CO (1 atm) at 65 °C in heptane to furnish the known compounds $Re_2(CO)_{10}$ (>93%) and $Cp^*Rh(CO)_2$ (>98%), as assessed by IR spectroscopy. No evidence for the presence of either $HRe(CO)_5$ or $H_3Re_3(CO)_{12}$ was observed in those reactions that were monitored by IR spectroscopy. Heating **4** in the absence of CO is accompanied by decomposition to $Re_2(CO)_{10}$ (<10%) and trace amounts of $Cp^*Rh(CO)_2$.

The kinetics for the fragmentation of **4** were studied in order to establish the role played, if any, by CO in this

(52) Beringhelli, T.; D'Alfonso, G.; Molinari, H.; Mann, B. E.; Pickup, B. T.; Spencer, C. M. *J. Chem. Soc., Chem. Commun.* **1986**, 796.
(53) Latten, J. L.; Hsu, G.; Henly, T. J.; Wilson, S. R.; Shapley, J. R. *Inorg. Chem.* **1998**, *37*, 2520.
(54) (a) Aime, S.; Milone, L.; Rossetti, R.; Stanghellini, P. L. *Inorg. Chim. Acta* **1977**, *25*, 103. (b) Hawkes, G. E.; Lian, L. Y.; Randall, E. W.; Sales, K. D. *J. Magn. Reson.* **1985**, *65*, 173. (c) Yeh, W.-Y.; Shapley, J. R.; Li, Y.-J.; Churchill, M. R. *Organometallics* **1985**, *4*, 767. (d) D'Agostino, M. F.; Miekuz, M.; Kollis, J. W.; Sayer, B. G.; Rodger, C. A.; Halet, J.-F.; Saillard, J.-Y.; McGlinchey, M. J. *Organometallics* **1986**, *5*, 2345. (e) Farrugia, L. J.; McDonald, N.; Peacock, R. D. *J. Cluster Sci.* **1994**, *5*, 341.
(55) Sanders, J. K. M.; Hunter, B. K. *Modern NMR Spectroscopy*; Oxford University Press: New York, 1993.
(56) Nakajima, T.; Shimizu, I.; Kobayashi, K.; Wakatsuki, Y. *Organometallics* **1998**, *17*, 262.
(57) (a) Masciocchi, N.; Sironi, A.; D'Alfonso, G. *J. Am. Chem. Soc.* **1990**, *112*, 9395. (b) Beringhelli, T.; D'Alfonso, G.; Freni, M.; Ciani, G.; Moret, M.; Sironi, A. *J. Chem. Soc., Dalton Trans.* **1989**, 1143.
(58) (a) Beringhelli, T.; Ciani, G.; D'Alfonso, G.; De Maldé, V.; Freni, M. *J. Chem. Soc., Chem. Commun.* **1986**, 735. (b) Haupt, H.-J.; Woyciechowski, M.; Flörke, U. *Z. Anorg. Allg. Chem.* **2004**, *592*, 153.
(59) The asymmetric Rh−C and Re−C bond distances exhibited by the face-capping CO groups in **7** are reminiscent of the bonding situation reported for the face-capping CO groups in the unsaturated trimetallic cluster $Cp^*_3Rh_3(\mu_3\text{-}CO)_2$ reported by Stone et al.; see: Bray, A. C.; Green, M.; Hankey, D. R.; Howard, J. A. K.; Johnson, O.; Stone, F. G. A. I. *J. Organomet. Chem.* **1985**, *281*, C12.
(60) Comstock, M. C.; Wilson, S. R.; Shapley, J. R. *Organometallics* **1994**, *13*, 3805.

reaction. Here UV−vis spectroscopy was employed, and the progress of each reaction was monitored by following the decrease in the absorbance of the 508 nm band of **4** under CO over the temperature range 326−361 K. Figure 7 shows the UV−vis spectral changes for the reaction of **4** in toluene at 333 K in the presence of 1 atm of CO (excess), with the inset depicting the least-squares fit for the first-order decay of **4** and the absorbance data.[61] The first-order rate constants for these reactions are quoted in Table 4. The effect of CO pressure, free-radical traps, and PPh_3 on the reaction was also explored (entries 6−9), and on the basis of the negligible changes in these rate constants vis-á-vis entry 2, we can rule out a rate-limiting step involving an associative attack of ligand on **4** and a decomposition sequence proceeding by a free-radical chain process.[62] The zero-order dependence of CO and the Eyring activation parameters ($\Delta H^{\ddagger}$ = 25.0(8) kcal/mol; $\Delta S^{\ddagger}$ = −2.6(3) eu) further rule out a rate-determining step involving dissociative CO loss from **4**.

The possibility of a rate-limiting loss of hydrogen in **4** was probed through the use of the dideutride cluster **4**-d_2, which was prepared from **1**-d_2 and **2**.[63] Our synthetic route to **1**-d_2 employed the published procedure for the synthesis of **1**-d_0 in benzene solvent, except that H_2 was replaced by D_2. The progress of the reaction was followed by IR spectroscopy and terminated upon consumption of the $Re_2(CO)_{10}$. The desired product was purified by recrystallization from hexane and then analyzed by ^{1}H NMR spectroscopy, employing 4,4′-di-*tert*-butylbiphenyl as an internal standard. The recorded spectrum confirmed the presence of ca. 17% of the **1**-d_0 and **1**-d_1 isotopomers in ca. a 14:86 ratio, respectively. These unwanted isotopomers presumably derive from the activation of the benzene reaction solvent and have also been observed by Beringhelli et al. during their preparation of **1**-d_2.[64] Changing the benzene photolysis solvent to cyclohexane reduced the amount of the unwanted isotopomers to ca. 4%,[65] and this material was used in the synthesis of **4**-d_2. Reaction of **1**-d_2 and **2** afforded **4**-d_2 in 25% isolated yield after crystallization from hexane. We specifically avoided the use of column chromatography in the purification step in order to prevent H/D exchange between the stationary support and the deuteride ligands in **4**-d_2.[20] ^{1}H NMR analysis of the **4**-d_2 in benzene-d_6 using the Cp* moiety as an internal reference allowed us to set an upper limit on the **4**-$d_{0,1}$ isotopomers at no more than 4% of cluster **4**. This material was sufficiently pure and was employed in the carbonylation kinetics.

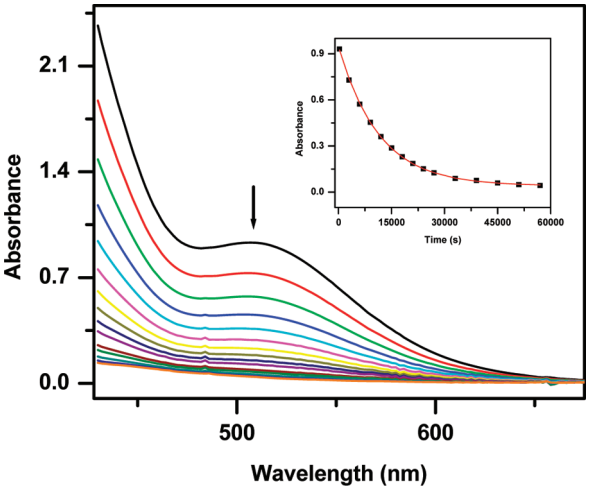

Figure 7. UV−vis spectral changes for cluster **4** in the presence of CO (1 atm; ca. 14 equiv CO per **4**) at 333 K in toluene. The inset shows the absorbance data versus time for the experimental data (black box) and the nonlinear regression fit of the first-order rate constant k (solid red line).

The reaction of **4**-d_2 under 1 atm of CO at 333 K was examined spectrophotometrically in a manner identical with that described above for **4**-d_0. Two independent reactions were conducted, and each exhibited well-behaved first-order decay curves for **4**-d_2, from which the average rate constant of 8.17(0.01) e^{-5} s^{-1} was obtained. This value compares well with the mean rate constant of 8.04(0.9) e^{-5} s^{-1} determined from the other experiments performed at 333 K using **4**-d_0 (entries 2−9, Table 4). The absence of a measurable isotope effect during the fragmentation of cluster **4** rules out a rate-limiting loss of H_2 (or D_2).[66,67] With dissociative processes based on CO and H_2 loss eliminated from consideration, a rate-determining step (RDS) that involves the opening of the cluster polyhedron to afford a diradical species appears reasonable on the basis of the totality of the kinetic data and the photochemical reactivity of **4** in the presence of chlorinated solvents (vide infra). A unimolecular reaction involving the opening of the cluster at the non-hydride-bridged Rh−Re bond would serve as a suitable RDS in the fragmentation of **4** (eq 3). The proposed Rh−Re bond scission in **4** also receives support by way of published kinetic and dynamic NMR studies, where polyhedral rearrangements involving metal−metal bond scission have been

(61) The carbonylation studies were conducted under pseudo-first-order conditions using excess CO relative to cluster **4**. CO concentrations in toluene were computed from the published solubility data: Basickos, L.; Bunn, A. G.; Wayland, B. B. *Can. J. Chem.* **2001**, *79*, 854.

(62) For reports on the inhibitory effect of 9,10-DHA and *p*-methoxyphenol on free-radical chain processes, see: (a) Lockhart, T. P.; Comita, P. B.; Bergman, R. G. *J. Am. Chem. Soc.* **1981**, *103*, 4082. (b) Narayanan, B. A.; Amatore, C.; Casey, C. P.; Kochi, J. K. *J. Am. Chem. Soc.* **1983**, *105*, 6351. (c) Narayanan, B. A.; Amatore, C.; Kochi, J. K. *Organometallics* **1984**, *3*, 802; **1986**, *5*, 926. (d) Mahoney, L. R. *J. Am. Chem. Soc.* **1966**, *88*, 3035.

(63) Given the preparative scale employed in the synthesis of **1**-d_2, it was impractical to isolate the desired d_2 isotopomer via column chromatography over D_2O-treated Florisil, as per the method described by Kaesz.[20] Recrystallization of the crude photoproduct from a minimal amount of hexane at low temperature afforded **1**-d_2 (predominant isotopomer) free from other rhenium byproducts.

(64) Beringhelli, T.; D'Alfonso, G.; Gobetto, R.; Panigati, M.; Viale, A. *Organometallics* **2005**, *24*, 1914.

(65) Our findings concerning the activation of the solvents benzene and cyclohexane in the preparation of **1**-d_2 are in accord with earlier seminal studies on the activation preference of arenes over alkanes at unsaturated metal compounds. For example, see: (a) Janowicz, A. H.; Bergman, R. G. *J. Am. Chem. Soc.* **1983**, *105*, 3929. (b) Jones, W. D.; Hessell, E. T. *J. Am. Chem. Soc.* **1993**, *115*, 554. (c) Arndtsen, B. A.; Bergman, R. G.; Mobley, T. A.; Peterson, T. H. *Acc. Chem. Res.* **1995**, *28*, 154. (d) Jones, W. D. *Top. Organomet. Chem.* **1999**, *3*, 9.

(66) For detailed studies dealing with the reductive elimination of hydrogen from metal clusters and kinetic isotope data (KIE) in such eliminations, see: (a) Bavaro, L. M.; Montangero, P.; Keister, J. B. *J. Am. Chem. Soc.* **1983**, *105*, 4977. (b) Keister, J. B.; Onyeso, C. C. O. *Organometallics* **1988**, *7*, 2364. (c) Safarowic, F. J.; Bierdeman, D. J.; Keister, J. B. *J. Am. Chem. Soc.* **1996**, *118*, 11805. (d) Pöe, A. J.; Sampson, C. N.; Smith, R. T.; Zheng, Y. *J. Am. Chem. Soc.* **1993**, *115*, 3174.

(67) For reports describing the use of deuterium kinetic isotope effects in the study of hydrogen transfer reactions and intramolecular hydride fluxionality in polynuclear systems, see: (a) Rosenberg, E. *Polyhedron* **1989**, *8*, 383. (b) Nevinger, L. R.; Keister, J. B. *Organometallics* **1990**, *9*, 2312. (c) Anslyn, E. V.; Green, M.; Nicola, G.; Rosenberg, E. *Organometallics* **1991**, *10*, 2600.

implicated in ligand substitution and ligand rearrangement.[68,69]

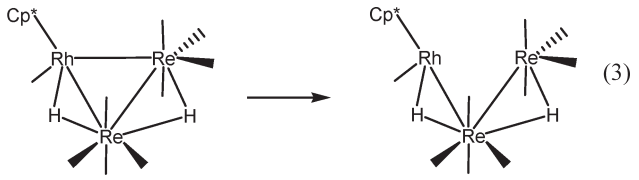

(3)

III. Thermal and Photochemical Decomposition of 4 in the Presence of Chlorinated Solvents. Whereas **4** decomposed in toluene in the absence of CO, the thermolysis behavior of **4** in the halogenated solvents CH_2Cl_2, $CHCl_3$, and CCl_4 under comparable conditions followed a different reaction course, with new ν(CO) bands at 2035 and 1917 cm^{-1} observed in those reactions monitored by IR spectroscopy. The spectroscopic signature of these ν(CO) bands is consistent with the presence of a *fac*-$Re(CO)_3$ moiety in the product, and ^1H NMR spectroscopy revealed the presence of a new Cp* singlet at δ 1.36. Quantitative IR spectroscopy established the presence of $Cp^*Rh(\mu\text{-}Cl)_3Re(CO)_3$ (**8**) in 82% yield after **4** and a solvent mixture composed of CH_2Cl_2/CCl_4 (1:1) were allowed to react overnight at ca. 45 °C. Since **8** could not be isolated by chromatographic techniques due to its irreversible binding to the stationary support, we had to resort to recrystallization in order to purify **8**. Following this protocol using hexane as the extraction and crystallization solvent, we were able to grow single crystals of **8**, whose molecular structure was subsequently confirmed by X-ray diffraction analysis (Figure 8). The molecular structure of **8** is similar to that of the structurally characterized bromo-bridged derivatives $Cp^*M(\mu\text{-}Br)_3Re(CO)_3$ (where M = Rh, Ir) and the iridium analogue $Cp^*Ir(\mu\text{-}Cl)_3Re(CO)_3$.[70,71] **8** exhibits a triply bridged confacial bioctahedral geometry, where the chlorine groups act as the common face-shared ligands. Both metal centers are coordinatively saturated according the effective atomic number (EAN) rule, provided the halides function as 3e-donating ligands. The internuclear Rh(1)···Re(1) bond distance of 3.2953(3) Å is significantly longer than those Rh−Re distances reported in clusters **4**−**7**, and this precludes any direct bonding interactions between the two metals. Bonding aspects have been theoretically addressed for sundry $L_3M(\mu\text{-}X)_3ML_3$ compounds as a function of the tethering ligand and the metal electron count.[72,73] In the case of **8**, application of the isolobal theory predicts that the union of the d^6-$[Cp^*Rh]^{2+}$ and d^6-$[Re(CO)_3]^+$ fragments by three chloride ligands will give rise to a filled set of low-energy d orbitals incapable of net Rh−Re bonding.

The structure of **8** is important, as it unequivocally establishes the activation of the chlorinated solvent in a sequence that presumably involves the diradical cluster $H_2RhRe_2Cp^*(CO)_9$, shown in eq 4. **8** is also obtained in low yield when solutions of **4** in the same halogenated solvents are irradiated overnight at 366 nm. Although not mechanistically studied, the photochemical route that furnishes **8** conceivably involves the formation of

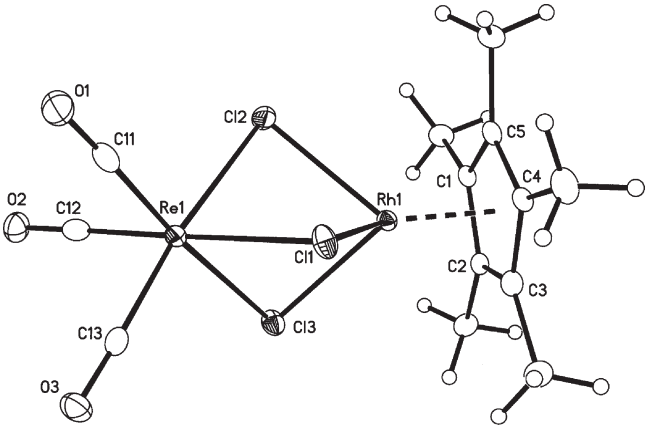

Figure 8. Thermal ellipsoid plot of the molecular structure of **8**, showing the thermal ellipsoids at the 50% probability level. Selected bond distances (Å) and angles (deg): Re(1)···Rh(1) = 3.2953(3), Cp*(centroid)−Rh(1) = 1.752(1); Rh(1)−Cl(1)−Re(1) = 83.64(2), Rh(1)−Cl(2)−Re(1) = 82.99(2), Rh(1)−Cl(3)−Re(1) = 82.91(2).

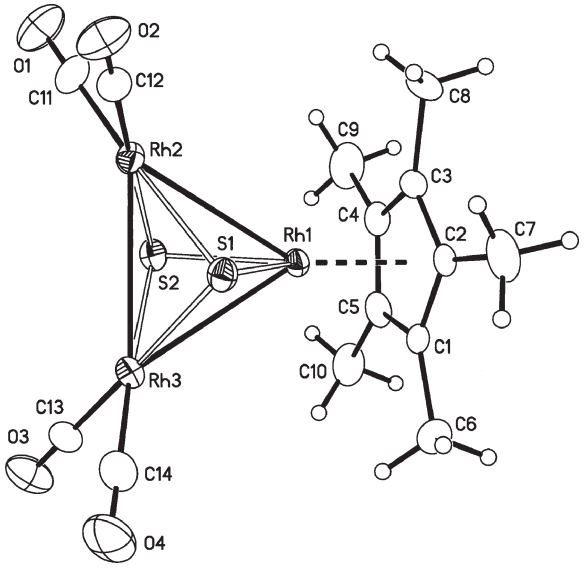

Figure 9. Thermal ellipsoid plot of the molecular structure of **9** showing the thermal ellipsoids at the 35% probability level. Selected bond distances (Å) and angles (deg): Rh(1)−Rh(3) = 2.9522(7), Rh(1)−Rh(2) = 2.9652(7), Rh(2)−Rh(3) = 3.0641(7), Rh(1)−S(1) = 2.310(2), Rh(2)−S(1) = 2.338(2), Rh(1)−S(3) = 2.339(2), Rh(2)−S(1) = 2.309(2), Rh(2)−S(2) = 2.337(2), Rh(3)−S(3) = 2.343(2), Cp*(centroid)−Rh(1) = 1.779(2); C(11)−Rh(2)−C(12) = 96.5(3), C(13)−Rh(3)−C(14) = 93.1(3).

(68) (a) Darensbourg, D. J.; Incorvia, M. J. *J. Organomet. Chem.* **1979**, *171*, 89. (b) Crowte, R. J.; Evans, J.; Webster, M. *J. Chem. Soc., Chem. Commun.* **1984**, 1344. (c) Richmond, M. G.; Kochi, J. K. *Inorg. Chem.* **1986**, *25*, 1334. (d) Tanaka, S.; Dubs, C.; Inagaki, A.; Akita, M. *Organometallics* **2004**, *23*, 317.

(69) As pointed out by one of the reviewers, the heterolytic cleavage of a Rh−Re bond in cluster **4** may also serve as the rate-limiting step in the thermal decomposition of **4**. While this manifold cannot be kinetically eliminated from consideration, we favor the homolysis of a Rh−Re bond in **4** and production of a biradical intermediate.

(70) da Silva, A. C.; Piotrowski, H.; Mayer, P.; Polborn, K.; Severin, K. *Dalton Trans.* **2000**, 2960.

(71) Wang, X.; Hammons, C.; Richmond, M. G. *Polyhedron* **2009**, *28*, 2294.

(72) Summerville, R. H.; Hoffmann, R. *J. Am. Chem. Soc.* **1979**, *101*, 3821.

(73) Our premise concerning the Rh···Re bonding in **8** is underscored by extended Hückel MO calculations on the model compound $CpRh(\mu\text{-}Cl)_3Re(CO)_3$, which afforded a reduced overlap population of −0.10 between the two metal centers.

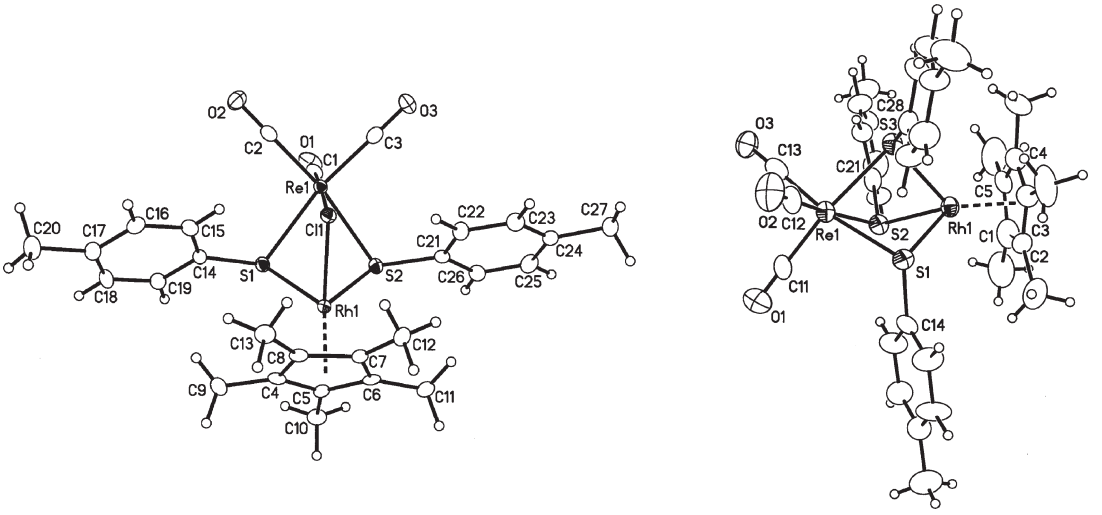

Figure 10. Molecular structures of **10** (left) and **11** (right) showing the thermal ellipsoids at the 50% and 35% probability levels, respectively. The hexane solvent molecule in the latter structure has been omitted for clarity. Selected bond distances (Å) and angles (deg) are as follows. For **10**: Re(1)···Rh(1) = 3.2894(4), Cp*(centroid)−Rh(1) = 1.786(2); Rh(1)−Cl(1)−Re(1) = 82.28(3), Rh(1)−S(1)−Re(1) = 84.34(3), Rh(1)−S(2)−Re(1) = 84.16(3). For **11**: Re(1)···Rh(1) = 3.325(1), Cp*(centroid)−Rh(1) = 1.799(5); Rh(1)−S(1)−Re(1) = 85.19(8), Rh(1)−S(2)−Re(1) = 85.15(7), Rh(1)−S(3)−Re(1) = 85.04(8).

metal-centered radicals that abstract chlorine atoms from the halogenated solvent. Optical excitation using near-UV light is expected to populate metal-based $\sigma\rightarrow\sigma^*$ manifolds within the cluster, which in turn can yield metal-centered radicals upon metal−metal bond homolysis.[74,75] The ability of such radicals to effectively abstract halogen and hydrogen atoms from suitable donors is a well-documented phenomenon.[76,77] Alternatively, **8** may be independently prepared in high yield by heating a 1:2 mol mixture of $[Cp^*RhCl_2]_2$ and $ClRe(CO)_5$, as shown in eq 4. We have successfully employed this protocol in the synthesis of the corresponding iridium derivative $Cp^*Ir(\mu\text{-}Cl)_3Re(CO)_3$.[71]

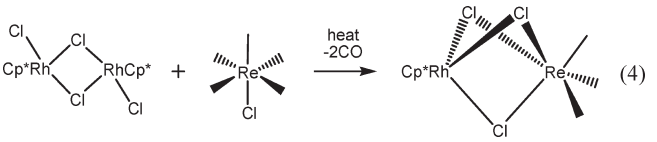

(4)

IV. Thermolysis Behavior of 4 in the Presence of Thiol Ligands. Due to current interests in biological mixed-metal hydrogenases and cluster-based systems capable of serving as models for industrial hydrodesulfurization catalysts, we next probed the reaction of **4** with thiols.[78] **4** reacts with H_2S-saturated benzene solutions at ca. 60 °C to give a single isolable product identified as $S_2Rh_3Cp^*(CO)_4$ (**9**). The IR spectrum showed three terminal carbonyl groups, while a single Cp* moiety was noted in the ^1H NMR spectrum consistent with the formulated structure. The ESI mass spectrum of **9** revealed a strong molecular ion at *m*/*e* 620.44 for the protonated cluster $[\mathbf{9} + H]^+$, in addition to a weaker peak at *m*/*e* 642.46 belonging to the sodiated species $[\mathbf{9} + Na]^+$. The metallic composition and the presence of the two $Rh(CO)_2$ moieties in **9** were subsequently established by X-ray diffraction analysis (Figure 9). The redistribution of rhodium atoms in this reaction is interesting, and the origin of the CO groups in the product must derive from the CO that is liberated from **4** during thermolysis. **9** consists of a triangular array of rhodium atoms that is face-capped by two sulfido groups; the cluster is electron precise based on a valence-electron count of 48e. The metallic core is best viewed as an equilateral triangle, since the Rh−Rh bond distances are approximately equal, exhibiting a mean distance of 2.9938 Å. The Rh−Rh bond distances in **9** compare well with those distances reported for the sulfido-capped clusters $[S_2Rh_3(CO)_6]^-$ and $S_2Rh_3(\mu\text{-}H)(cod)_2(PHBu^t_2)_2$.[79,80] The Cp* ligand is orthogonal to the metallic frame on the basis of the angle of 91.3(2)° formed from the planes defined by the C(1)−C(5) ring carbons and Rh_3 core. The remaining bond distances and angles are unremarkable and require no comment.

The reaction between **4** and *p*-methylbenzenethiol was also investigated. Heating **4** in the presence of a slight excess of *p*-methylbenzenethiol at 55 °C in benzene leads to the formation of the single new product **11**, as assessed by TLC analysis of the final reaction solution. Interestingly, parallel

(74) (a) Tyler, D. R.; Levenson, R. A.; Gray, H. B. *J. Am. Chem. Soc.* **1978**, *100*, 7888. (b) Delley, B.; Manning, M. C.; Ellis, D. E.; Berkowitz, J.; Trogler, W. C. *Inorg. Chem.* **1982**, *21*, 2247.

(75) For some recent time-resolved photophysical reports that demonstrate optically promoted metal−metal bond homolysis in polynuclear clusters, see: (a) Nijhoff, J.; Bakker, M. J.; Hartl, F.; Stufkens, D. J.; Fu, W.-F.; van Eldik, R. *Inorg. Chem.* **1998**, *37*, 661. (b) Bakker, M. J.; Hartl, F.; Stufkens, D. J.; Jina, O. S.; Sun, X.-Z.; George, M. W. *Organometallics* **2000**, *19*, 4310.

(76) (a) Wrighton, M. S.; Ginley, D. S. *J. Am. Chem. Soc.* **1975**, *97*, 2065. (b) Ginley, D. S.; Wrighton, M. S. *J. Am. Chem. Soc.* **1975**, *97*, 4908. (c) Hepp, A. F.; Wrighton, M. S. *J. Am. Chem. Soc.* **1981**, *103*, 1258. (d) McCullen, S. B.; Brown, T. L. *J. Am. Chem. Soc.* **1982**, *104*, 7496. (e) Hanckel, J. M.; Lee, K.-W.; Rushman, P.; Brown, T. L. *Inorg. Chem.* **1986**, *25*, 1852. (f) Tyler, D. R.; Goldman, A. S. *J. Organomet. Chem.* **1986**, *311*, 349. (g) Lee, K.-W.; Hanckel, J. M.; Brown, T. L. *J. Am. Chem. Soc.* **1986**, *108*, 2266. (h) Tenhaeff, S. C.; Covert, K. J.; Castellani, M. P.; Grunkemeier, J.; Kunz, C.; Weakley, T. J. R.; Koenig, T.; Tyler, D. R. *Organometallics* **1993**, *12*, 5000.

(77) For detailed reports on hydrogen-atom abstraction via electrochemically generated metal radicals, see: (a) Kuchynka, D. J.; Amatore, C.; Kochi, J. K. *Inorg. Chem.* **1986**, *25*, 4087. (b) Kuchynka, D. J.; Amatore, C.; Kochi, J. K. *J. Organomet. Chem.* **1987**, *328*, 133.

(78) (a) Rees, D. C. *Annu. Rev. Biochem.* **2002**, *71*, 221. (b) Stiefel, E. I., Matsumoto, K., Eds. *Transition Metal Sulfur Chemistry: Biological and Industrial Significance*; American Chemical Society: Washington, DC, 1996.

(79) Galli, D.; Garlaschelli, L.; Ciani, G.; Fumagalli, A.; Martinengo, S.; Sironi, A. *J. Chem. Soc., Dalton Trans.* **1984**, 55.

(80) Arif, A. M.; Hefner, J. G.; Jones, R. A.; Koschmieder, S. U. *Polyhedron* **1988**, *7*, 561.

reactivity experiments employing **8** and *p*-methylbenzenethiol afforded compounds **10** and **11** as the principal reaction products. These last two compounds are also observed by TLC in those reactions between **4** and thiol ligand conducted in CH_2Cl_2. Crude reaction mixtures containing **10** and **11** are easily driven to the latter product in good yield upon further addition of *p*-methylbenzenethiol. **10** and **11** were isolated as air-stable solids by column chromatography over silica gel and characterized by IR and ^{1}H NMR spectroscopy, ESI mass spectrometry, and X-ray crystallography. Both compounds exhibit two strong ν(CO) stretches associated with the $Re(CO)_3$ moiety, albeit appropriately shifted to lower energy relative to the corresponding chloride-bridged dimer **8** due to the presence of the stronger donor thiolate donor groups. While no molecular ion was found in the ESI mass spectrum of **10**, the peak recorded at *m*/*e* 755.00 is consistent with the formation of $[\mathbf{10} - Cl]^+$; **11** displayed two strong peaks in the mass spectrum at *m*/*e* 900.93 and 754.95 for the sodiated species $[\mathbf{11} + Na]^+$ and $[\mathbf{11} - SC_6H_4Me]^+$, respectively. Figure 10 shows the molecular structures of **10** and **11**, and given their similarity, only the salient features will be discussed. To our knowledge, **10** and **11** represent the first structurally characterized sulfido-bridged heterobimetallic Cp*RhRe compounds possessing a confacial bioctahedral motif. The overall molecular geometry of each compound is similar to that of **8**, with the internuclear Rh(1)···Re(1) distances in **10** (3.2894(4) Å) and **11** (3.325(1) Å) not significantly different vis-á-vis that distance in **8**. The bridging SC_6H_4Me-4 ligands in **10** and **11** adopt a disposition that is basically parallel to the plane containing the Cp* ring carbon atoms and perpendicular to the Rh(1)···Re(1) vector.

Conclusions

$H_2Re_2(CO)_8$ (**1**) reacts with $Cp^*Rh(CO)_2$ (**2**) to yield the new cluster compounds $H_2RhRe_2Cp^*(CO)_9$ (**4**), $HRh_2ReCp^*_2(CO)_6$ (**5**), and $HRhRe_3Cp^*(CO)_{14}$ (**6**). The nature of the rhodium starting material is important, and substitution of **3** in place of **2** affords clusters **4**, **5**, and $H_2Rh_2Re_2Cp^*_2(CO)_8$ (**7**). The reactivity of **4** has been explored in detail and unexpectedly found to decompose under relatively mild conditions to give fragmentation products whose composition is dependent on the nature of the trapping ligand present and reaction solvent. The fragmentation kinetics of **4** under CO have been investigated, and the data support a unimolecular rate-determining step that involves the opening of the cluster polyhedron through homolytic scission of one of the Rh−Re bonds in **4**. Cluster **4** undergoes fragmentation in the presence of the halogenated solvents CH_2Cl_2, $CHCl_3$, and CCl_4 to give the heterobimetallic halide-bridged species $Cp^*Rh(\mu\text{-}Cl)_3Re(CO)_3$ (**8**).

Acknowledgment. Helpful comments from Prof. John Shapley are acknowledged and much appreciated. We also thank the reviewers concerning their comments on the VT NMR behavior of cluster **7**. Financial support from the NSF (C.J.C.) and Robert A. Welch Foundation (Grant B-1093-MGR) is greatly appreciated, while the NSF-MRI program grant CHE-0320848 is gratefully acknowledged for support of the X-ray diffraction facilities at San Diego State University. X.W. acknowledges support by the U.S. Department of Energy, Office of Science, under Contract No. DE-AC05-00OR22725 managed by UT Battelle, LLC. The expert assistance of Dr. Yongxuan Su in obtaining the reported mass spectral data is acknowledged.

Supporting Information Available: A figure giving VT ^{1}H NMR profiles of cluster **4** and CIF files giving crystallographic data. This material is available free of charge via the Internet at http://pubs.acs.org.